SLAC-139 (Revised)
(TH),(EXP),(ACC)
UC-28

DESCRIPTION AND PHYSICS PROGRAM OF THE PROPOSED RECIRCULATING LINEAR ACCELERATOR (RLA)

STANFORD LINEAR ACCELERATOR CENTER

STANFORD UNIVERSITY

Stanford, California 94305

PREPARED FOR THE U.S. ATOMIC ENERGY

COMMISSION UNDER CONTRACT NO. AT(04-3)-515

February 1972

Printed in the United States of America. Available from National Technical Information Service, U. S. Department of Commerce, 5285 Port Royal Road, Springfield, Virginia 22151.
Price: Printed Copy $3.00; Microfiche $0.95.

DESCRIPTION AND PHYSICS PROGRAM OF THE PROPOSED

RECIRCULATING LINEAR ACCELERATOR

(RLA)

The following people have contributed to the work described in this document:

M. A. Allen
J. Ballam
S. J. Brodsky
K. L. Brown
L. E. Brown
W. O. Brunk
*E. E. Chambers (HEPL)
J. K. Cobb
*E. D. Courant (BNL)
K. F. Crook
W. Davies-White
S. D. Drell
D. Edwards (NAL)
R. J. Fuendeling
G. E. Fischer
*E. Freytag (DESY)
*A. A. Garren (LRL)
L. Genova
R. S. Gould
*K. Halbach (LRL)
F. F. Hall
R. H. Helm
W. B. Herrmannsfeldt
H. A. Hogg
T. M. Jenkins
R. Jeong
J. Jurow
R. F. Koontz
L. J. Kral
C. J. Kruse
*G. R. Lambertson (LRL)
M. J. Lee
A. V. Lisin
J. V. Lebacqz
G. A. Loew
K. B. Mallory
R. H. Miller
P. L. Morton
*D. Mohl (LRL-CERN)
R. B. Neal
C. W. Olson
W.K.H. Panofsky
*C. Pellegrini (Frascati)
J. R. Rees
B. Richter
D. B. Robbins
R. M. Rowe
*M. Sands (U.C. Santa Cruz)
E. J. Seppi
*A. Sessler (LRL)
*L. Smith (LRL)
E. L. Stockbridge
R. L. Stringall
*L. Teng (NAL)
R. E. Taylor
A. A. Tseng
D. Walz
H. A. Weidner
K. M. Welch
P. B. Wilson
B. M. Woo

*The people from outside institutions whose names are preceded by an asterisk participated in a two-week summer study, held at SLAC, June 7th - 18th, 1971, which mainly examined some of the overall beam dynamics problems involved in the proposal.

ABSTRACT

A method of approximately doubling the energy of the SLAC Accelerator by recirculation of the beam and reinjection into the machine for a second pass is described. The recirculator could also be used for high duty cycle (up to 6%) experiments at the recirculating energy by storing the beam and extracting about 1% of the electrons per revolution. Recirculation will initially occur at an energy of 17.5 GeV. Beam losses of ~125 MeV due to synchrotron radiation would be compensated by 2 sectors (666 ft) of standard accelerator sections operating at the accelerator frequency (2856 MHz). These sectors will be pulsed at a repetition rate of 43,500 pulses per second corresponding to the recirculating period of about 23 microseconds. The beam will be stored for 2.8 milliseconds (approximately 122 revolutions around the 6900 meter storage path); this is the time interval between the normal pulses of the accelerator. Using this method, the energy of the SLAC accelerator could be increased initially to about 42.5 GeV. The recirculator is designed to permit later increase of the storage energy to 25 GeV by the use of superconducting accelerator sections to restore the synchrotron energy loss. Then, assuming that a proposed program to replace the present 30 MW klystrons powering the accelerator with 60 MW models has been completed, the maximum beam energy would become 60 GeV.

Upon completion of the proposed recirculation system the increased beam energy and duty cycle will greatly enhance its utility in particle physics research. A discussion of some of the physics opportunities which would become available is given.

TABLE OF CONTENTS

LIST OF TABLES

LIST OF FIGURES

I. INTRODUCTION

Various methods of upgrading the energy and duty cycle of the SLAC accelerator have been studied during the past two years. These schemes have included the simple (in principle) procedure of adding more rf power to the existing accelerator, the complex and still speculative idea of replacing the present accelerator with a superconducting machine operating at $1.85^{\circ}K$, and the Recirculating Linear Accelerator (RLA) scheme described in this report.

The first method, based on adding rf power, suffers from the basic fact that beam energy in a linear accelerator increases only as the square root of the input power. For example, suppose that the goal is to double the present beam energy. This objective could be achieved only by increasing the input rf power by a factor of four, a costly undertaking in terms of both initial and operating costs. For this reason, the practical, or "realistic," versions of this method which have been recently envisaged, have been limited to potential energy increases of 40%.

The superconducting accelerator is a promising method of obtaining a large increase in linac duty cycle and energy. Studies at SLAC[1] have projected beam energies almost 5 times that of the present machine and duty cycles 100 times as high. However, up to the present time, the gradients required for this achievement have been obtained only in a few carefully prepared test cavities; actual operation of even very short accelerators at these high gradients has not yet been accomplished. Work continues in this field at several laboratories but many technological problems remain to be solved before a multi-GeV superconducting linear accelerator could be built. Thus, even if the conversion of the SLAC accelerator to a superconducting machine becomes technically feasible, it is not clear that it could happen early enough to make such an endeavor competitive from the Physics point of view.

The advantage of the Recirculating Linear Accelerator (RLA) described in this report is that it provides a relatively inexpensive way of approximately doubling the beam energy of the SLAC accelerator, bringing it into the 40 GeV range. In another mode of operation, it permits operation with ~100 times the present duty cycle at the present level of beam energy. This method of upgrading the SLAC machine is relatively less costly because it achieves the energy increase by utilizing the presently available accelerator and rf system for two successive acceleration passes. The beam is stored in a recirculator for the time interval (2.8 milli-seconds) between the normal pulses of the accelerator. Storage is followed by the reinjection of the beam into the machine for a second acceleration.

New accelerator sections are required in the recirculator to restore the energy lost by synchrotron radiation during beam storage. Initially, two sectors (666 ft) of conventional accelerator structure will provide sufficient energy to permit storage of a 17.5 GeV beam. Later, the energy of the stored beam can be increased to 21 GeV by providing two additional accelerator sectors or to 25 GeV by the use of superconducting accelerator sections[2,3] in place of or in addition to the conventional accelerator structures in the loop.

As discussed later in this report, the recirculation system can be accommodated on the SLAC site without serious difficulties. Estimated construction time is reasonable and the installation of the recirculator can be accomplished with only a few months loss in beam operation of the present SLAC accelerator. Upon completion of the recirculation system, the increased beam energy and duty cycle of the SLAC machine will greatly enhance its utility in particle physics research. Some of the physics opportunities which become available at these higher energies and duty cycles are discussed in the next section.

II. HIGH ENERGY PHYSICS OBJECTIVES

A. Introduction and Summary

The potential impact of an increase in energy and duty cycle of the two-mile accelerator can be understood by considering SLAC's research program of the past four years. This program has made it abundantly clear that the study of particle physics via electron and photon scattering experiments plays an essential and unique role in the investigation of the structure of the hadrons. The importance of such experiments derives from the fact that the electromagnetic interaction is well understood, can be well treated in the formal analyses and exhibits a local, point-like nature. The known electromagnetic field generated during the electron's scattering which interacts with the electromagnetic current of the hadron target can thus probe the structure of the nucleon at arbitrarily small distances. This is in sharp contrast to hadron-hadron scattering, in which the basic interaction between the target and beam particles is both unknown and diffuse, so that it is difficult to isolate the target particle.

The measurements of inelastic electron scattering performed at SLAC in the past few years have given evidence of a scale-invariant behavior of the proton and neutron structure functions which strongly hints at a rich substructure within the nucleon itself. Complementary to these processes are the other electromagnetic probe experiments such as hadron production in electron-positron annihilation and wide-angle pair production in hadron-hadron collisions. The present exciting results from all these areas of electromagnetic interactions confirm that the detailed study of electron and photon scattering plays a vital role in developing an eventual understanding of the elementary particles.

Electron or muon scattering experiments can be looked at as (virtual) photoproduction experiments in which the photon mass can be controlled by varying the

energy and angle of the scattered lepton. This possibility of "tuning" the photon's mass is a unique feature of lepton-induced reactions. In addition, the polarization of the incident photon (real or virtual) may also be controlled experimentally. The scattering experiments performed at SLAC to date are inclusive measurements in which the scattered electron is detected and all available hadron channels are summed over. They are in effect total cross section measurements in which the virtual photons have a particular mass and polarization. The projected increase in energy obtained with the RLA will greatly extend the kinematic range covered by these measurements and more than double the energy that can be transferred to the target hadron. In particular one is anxious to learn if the proton continues to scatter as if individual point-like constitutents are contributing incoherently. The high-intensity electron beam (up to 10^6 times more intense than the corresponding muon beams currently proposed at NAL) will allow detailed, precise measurements of the electroproduction cross sections and will be a necessary complement to the gross measurements possible at NAL at still higher energies.

The increased duty cycle will make feasible more complex experiments using coincidence techniques in which individual final-state hadronic channels can be explored in much the same way as in present hadron-hadron experiments, but, again, as a function of the virtual photon mass. The detailed information that can be obtained in this way is analogous to the study of differential cross sections—momentum distributions, multiplicities, etc., in hadron physics relative to total cross section measurements.

A study of the correlations and distributions of the final hadronic particles in these processes will be essential to the understanding of the observed scaling laws and of the fundamental structure of the proton — whether, for example, the proton scatters as a "liquid" medium with long-range internal order or as a "gas" medium with none.

The study of reactions in which strongly interacting particles are produced by high-energy gamma rays (photoproduction) has been a major field of research at SLAC. These experiments have contributed directly to our understanding of the dynamics of the strong interaction, both in their own right and because they complement experiments done at other laboratories, such as Brookhaven or CERN, with incident proton and meson beams. The improvements proposed here for the SLAC machine will allow a great extension of this work. An increase in the duty cycle of the accelerator in the 15 to 20 GeV energy region by a factor of about 100 should provide an increase of the same factor of 100 in the amount of data already obtained on multiparticle momentum and angle correlations in photoproduction reactions. Most of the work to date in this multiparticle field has been devoted to the various vector-meson production reactions which have relatively large cross sections. The increase in data rate allowed by the improvement in duty cycle will allow experiments to be done on reactions with smaller cross sections, and hence broaden the spectrum of experiments which complement the work done in the same energy range at Brookhaven and CERN.

At the higher energies the approach of total photon cross sections to their asymptotic limits as well as their ratios for different targets can be studied with great accuracy and detail. Recent Serpukhov results on the increase of K^+ total cross sections between 20 and 60 GeV emphasize the importance of accurate and detailed studies of the approach to Pomeranchuk limits in this energy range. As another example, very inelastic photoproduction of massive μ-pairs can be studied for scaling laws similar to those found in deep inelastic scattering of electrons by protons. In comparison with the production of massive μ-pairs in proton-proton collisions, it is possible to learn about the fundamental photon structure. Also, it will be possible to study Compton scattering — both elastic as a probe of Regge

and of vector dominance predictions, and inelastic scattering in inclusive experiments at large momentum transfers, viz., $\gamma + p \rightarrow \gamma +$ anything, in order to test predictions based on point-like constituents in the proton.

In photoproduction the use of a polarized photon beam is important because it provides the only practical boson beam with spin. Consequently, it is a unique tool in the study of the spin dependence of meson processes. SLAC has been very successful in developing such a beam and experiments with it have shown that ρ^0 photoproduction tends to conserve the s-channel helicity of the photon; i.e., the spin of the rho is along its direction of motion. The polarized photon beam also allows a clean separation of the interactions due to exchange of natural and unnatural particles or "trajectories"; in this case only one beam is necessary as opposed to the hadron beam case where cross sections from different types of reactions are needed to make the separation.

Many interesting hadron experiments have also been done at SLAC. This has been especially true for processes in which the cross sections are high enough so that the experiment is limited by the rate capabilities of the particular data-acquisition system (including the off-line computer as well as the detector itself) rather than the secondary beam intensity. SLAC can continue to be a very important source of secondary hadron beams to supplement and complement the proton accelerators.

In particular, the high repetition rate at SLAC permits application of an important new technology in the area of fast-cycling bubble chambers operating in a triggered mode. Also, the secondary hadron beams produced by photons at SLAC have characteristic compositions which can be put to favorable use. For example, the neutral kaon beams are much more free from background neutrons than similar beams from proton accelerators; furthermore, at higher electron

energies one expects to also produce anti-neutron beams in the forward direction with a favorable $\bar{n}/n$ ratio. Finally the study of low cross section hadron processes induced by pions, such as backward-produced pion resonances, quasi two-body final states involving high-mass nucleon resonances, etc., will be possible for the first time at SLAC since the full pion intensity (10^5/sec) in the energy range 10-20 GeV will be utilized.

For their present role in probing the hadronic structure, electrons and muons are well understood as point particles with known electromagnetic interactions. Whether there are just two such point leptons as the muon and electron, identical in all properties except for their masses and separately conserved lepton numbers, or they are members of a larger family, is one of particle physics' greatest puzzles. Can one identify any differences in their interactions with hadrons? All new accelerators probing new energy and mass domains will have as a high priority the search for new heavy leptons, and SLAC's unique contribution to this search will be the electromagnetic production modes. Anything with charge and/or magnetic moment can be pair-produced and with higher energies at SLAC one can extend the search for new and more massive particles. No one can anticipate the results obtained from new particle searches and, in particular, a priori no one knows the dominant and identifiable production modes and their fundamental significance for understanding the structure of elementary particles and their interaction.

The key beam parameters of the RLA are summarized in Table I. For a detailed explanation of this table, the reader is referred to Section III. The beam intensity will be of the order of 10^{14} electrons per second. By contrast, the estimated muon flux from the 500 GeV NAL proton beam will be approximately 10^6 muons per second at 100 GeV; this limit is set primarily by the beam halo of other secondary particles. The electron beam attainable from neutral pion decay at NAL

is expected to be between 10^7 and 10^8 electrons per second. Thus, for purposes of electromagnetic physics, there is an intensity ratio of at least six orders of magnitude in favor of the recirculating SLAC accelerator.

B. General Areas of Research

Deep Inelastic Processes:

The deep inelastic electron scattering results at SLAC have clearly shown that there are very large reaction rates as well as many contributing channels. To be more specific, consider the process shown in Fig. 1 in which an electron scatters inelastically and is detected after transferring energy ν and invariant four-momentum square q^2 to a target nucleon (hadron of mass M). For values of $\nu/M > 1$ and $q^2/M^2 > 1$, i.e., the deep inelastic region, the data indicate cross sections much larger than the partial cross sections to individual nucleon ground and resonance states shown by Fig. 2. With increasing q^2, the resonance bumps disappear into the large continuum tail and the scattering behaves as if it occurs from point-like constituents (anticipated by Bjorken and called "partons" by Feynman) in the proton, each contributing independently of the others, just as the individual electrons add incoherently to make up the atomic cross section for highly inelastic scattering from atoms.

The structure functions for the inelastic cross sections, which are the analogues of the rapidly decreasing elastic form factors, are observed to behave as universal functions of the dimensionless variable $2M\nu/q^2$ as first conjectured by Bjorken and to remain large in the presently accessible range of ν and q^2. With a higher energy beam in the 40-50 GeV region, it will be possible to greatly extend the range of ν (from 18 to ~ 40 GeV) and to explore far into this deep inelastic scattering range. What new happens as we explore this unknown region? Does "scaling" remain valid? Quantitative measurements to test the extension of this universal behavior

with all its implications for point-like currents or "partons" within the nucleon is of enormous importance. What will also be very important to measure, and to begin to understand, is the detailed structure of the deep inelastic process and to learn what the properties (numbers, charges, types) of these partons are. For example the separation of $\sigma_L(\nu, q^2)$ and $\sigma_T(\nu, q^2)$ (the scalar and transverse total inelastic virtual photon cross sections) is important in order to determine the parton spin. It requires large angle lepton scattering and puts correspondingly severe requirements on the event rate. Thus this experiment can only be done with SLAC intensities. To find additional clues for answering these questions, one needs to study the distribution and multiplicities of secondary particles emerging from the proton in Fig. 1, as well as the dominant individual final-state channels, their mass distributions and dependence on momentum transfer. These are the analogues of the richly rewarding studies with incident baryon and pion beams that have paced the understanding of hadron dynamics and are the processes that the recirculating accelerator with a higher duty cycle would first open to our view.

The present single arm experiments have already uncovered much of interest. With good duty cycle in the 15-25 GeV region at SLAC, one could explore this region without expensive and major new developments in the experimental areas. Indeed, the inelastic electron scattering technique for exciting or pionizing the proton to individual final channels has several unique charms. For example, by varying the kinematics of the scattered electron in Fig. 1, the broad regions of q^2 and ν can be mapped out. In contrast, the hadron processes allow only variation of the incident energy but not of the mass of the incident particle. Polarization information can also be obtained from inelastic electron scattering, since the polarization of the "virtual" exchanged photon in Fig. 1 can be controlled and varied by the scattering kinematics. The improvement of the duty cycle by a factor of roughly

100 at present energies means that the event rates can be increased comparably. This will allow measurement of smaller cross sections to specific channels.

Very inelastic scattering of real photons will also shed important new light on the constituent structure of both protons and photons. The very inelastic Compton effect, $\gamma + p \longrightarrow \gamma + X$ at very large transverse momentum transfer as illustrated in Fig. 3, may be large and observable, and its behavior can extend the ideas of the parton model to very virtual parton states in the proton. This will cast light on the validity of the model in this new application. It is predicted to be a large and measurable process at high energies. Also, very inelastic photoproduction of massive μ pairs in the reaction $\gamma + p \longrightarrow (\mu\overline{\mu}) + X$ is predicted to be large and observable (see Fig. 4). This is a measurement that requires good duty cycle for detecting the muons in coincidence. Conditions for avoiding the Bethe-Heitler peak have been studied, for the first time, and observed scaling properties in this cross section will probe the parton structure of photons themselves.

Comparison of μ-p and E-p Inelastic and Elastic Scattering:

The recent SLAC experiment on muon-proton inelastic scattering showed no experimentally significant q^2 dependent difference between muon-proton and electron-proton inelastic scattering. However, within the overall normalization uncertainty the muon cross sections are systematically lower than the electron cross sections. An identical effect has been found in the comparison of muon-proton and electron-proton elastic scattering. Thus, it would appear to be very fruitful to carry out a new careful comparison at moderate q^2 values (0.1 to 2.0 $(GeV/c)^2$) of muon-proton and electron-proton inelastic scattering, as well as extending these comparisons to as high a q^2 as possible (8-10 $(GeV/c)^2$). Particular attention must be paid to normalization questions such as the relative normalization between the muon and electron experiments. Finally, the muon statistics should be improved

by a factor of twenty. Such an experiment can be carried out with a good duty cycle at SLAC for which the muon beam would be an improved high intensity version of the small phase space muon beam already used at SLAC. The electron beam would be the SLAC primary electron beam. The same apparatus would be used for the muon experiment and the electron experiment. Such an experiment can only be carried out at SLAC. First, the primary electron beam is necessary. Second, it is necessary to have a muon beam with a small phase space, sharp cutoff and low halo. It appears to be very difficult, if not impossible, to make such a muon beam at a proton machine.

In the recently completed comparison of muon-proton and electron-proton inelastic scattering, all hadronic channels were summed together. However, if one wishes to test the speculation that there may be a special interaction between the muon and hadrons, then a channel-by-channel comparison of muon-proton and electron-proton inelastic scattering is needed. Such an experiment obviously requires at least partial identification of the hadronic states produced in the inelastic interaction. Again, this requires a good duty-cycle accelerator and small phase space muon and electron beams.

Another possibility is to work with "virtual" muon beams, where the muons are produced by the Bethe-Heitler process from a photon beam (see Fig. 5). The event is triggered on the spectator muon. It is expected that the number of μ pairs per incident particle, per GeV, would be $\sim 10^{-5}$ at 42.5 GeV. The observation of wide angle muon pairs (including inelastic processes) will also be a test of QED since highly-virtual muons are involved.

New Particles and Heavy Lepton Search:

There will be great interest in experimental searches for new particles (or "objects") that are electromagnetically pair produced. An obvious way to search

for heavy lepton pairs is to use e^-e^+ colliding beams, but these experiments should be complemented by real photons. In addition, the center-of-mass energy of a 42.5 GeV electron beam is 9 GeV higher than any colliding beams now being built. At the lower energies, searches for these leptons at SLAC have in the past been hampered by the difficulty of separating these presumably short-lived leptons from the copious background of pair produced electrons and muons. A good duty cycle will considerably reduce this problem and enable coincidence techniques to be used in the search. Using wire spark chambers and scintillators, the search can be carried out by looking for either charged or neutral particles from the special decay modes of the heavy lepton.

Vector Boson Searches:

A further possibility is to observe intermediate boson production by measuring the spin of the produced muons, and taking advantage of the time structure of the SLAC beam. This is done by capturing a muon into a dc magnetic field and measuring the time distribution of the decay electrons. This technique, combined with the high intensity of the SLAC accelerator, can be used to investigate a number of highly fundamental questions such as:

1. Production of virtual W pairs leading to muon pair production via exchange of a neutrino. The diagram shown in Fig. 6a should interfere with the μ pair production by conventional Bethe-Heitler processes and should also result in characteristic correlations of the polarizations of the two produced muons. The counting rates are high enough at intensities attainable with the RLA to make these investigations worthwhile.

2. A single μ meson can be produced through the diagram shown in Fig. 6b. Since in this diagram only one of the W's is real, the cross section of such a process will hold up to a measurable value for W masses higher than those subject to investigation at other accelerators, using other processes. Again, the polarization of the μ produced in this process should yield a characteristic signature.

High q^2 Experiments on Lepton Conservation:

The conservation of lepton numbers is based primarily on experiments in which the four-momentum transfer to the lepton is small. For example, the four-momentum transfer to the leptons in the forbidden reaction $\mu \longrightarrow e + \gamma$ is very small. Therefore, one may speculate as to how well lepton number conservation will be maintained when the four-momentum transfer to the lepton is large, so that the internal structure of a particle can be probed in detail locally. Electron-positron colliding beams are beginning to provide large, time-like, or energy-like four-momentum transfer tests of lepton conservation. Tests with large space-like momentum transfers should also be made systematically and carefully. Below are listed a number of reactions which would test lepton conservation in its various forms:

$\mu + p \rightarrow e + p$ $\quad q^2 > 1\ (GeV/c)^2$

$e + p \rightarrow \mu + p$ $\quad q^2 > 1\ (GeV/c)^2$

$e + p \rightarrow$ hadrons only

$\mu + p \rightarrow$ hadrons only

$\mu + p \rightarrow e +$ hadrons (no μ)

$e + p \rightarrow \mu +$ hadrons (no e)

Photoproduction:

A full experimental program on photoproduction to study quantitative details of momentum and angular distributions will complement analogous studies at CERN and Brookhaven with incident protons, and with incident mesons in the secondary beams at SLAC and elsewhere. (It is worth noting that the steep energy dependence of secondary particle yields at BNL and CERN makes it difficult to do experiments with secondary beams near the maximum possible energies. Thus, while these proton machines have peak energies of around 30 GeV, almost all of the meson

induced reactions studies have been at energies less than or equal to 16 GeV.) A 15 to 20 GeV good duty cycle SLAC machine is thus a good complement in photoproduction to meson physics at a 30 GeV proton machine. Many of these experiments can be done with polarized photon beams produced by coherent bremsstrahlung on diamond crystals or by selective attenuation in oriented graphite crystals. By measuring azimuthal distributions of photoproduced particles relative to the scattering planes defined by the incident photon and the recoil target nucleon, one can distinguish normal from abnormal parity exchanges in a t (or momentum transfer) channel description of two-body interactions like $\gamma + p \rightarrow \pi^+ + n$, $\pi^o + p$, $\eta + p$, $K + \Lambda$, $K + \Sigma$, etc. This can be done in both the near forward and near backward directions where meson and baryon exchange, respectively, should dominate.

The rates of data gathering in the 15-20 GeV range will be roughly 2 events/second/μb — a reputable rate since most cross sections are in the .01 - μb range (with the exception of diffractive ρ_0 production which is $\sim 10\,\mu$b). This could lead to very efficient photoproduction survey work by the streamer chamber in which 4 pictures per second (each having an event) could be taken with only a 2% e^+e^- pair contamination. It also opens up the use of large wire chamber spectrometers to photoproduction studies.

The use of high intensity polarized beams which can now be tagged so as to obtain precise energy information on the incoming photon will be of great importance. Using 0.003 in. diamond crystals, the multiple scattering is low enough so that collimation equivalent to a $\Delta E/E \sim 6\%$ is achievable without tagging and 0.2% with tagging. Calculations show that for a 20 GeV electron beam, one can obtain 3×10^8 photons/sec of 15 ± 0.9 GeVwith a 45% polarization. This is $\sim 10^4$ times the intensity of <u>all</u> photons (unpolarized) between 100 and 200 GeV in beams proposed for NAL.

At the higher energies the back scattered laser technique can be used to produce photons having up to one-half of the electron energy. With the development of high repetition rate lasers, the experiments on vector meson photoproduction can be extended using the streamer chamber technique.

This facility should also make possible a further polarization dependent measurement, the evaluation of the Drell-Hearn sum rule which relates scattering of photons and nucleons with parallel and antiparallel spin to the nucleon magnetic moment. This measurement which requires polarized photons and a polarized proton target, will test the high energy behavior of the scattering amplitudes together with their analyticity (through unsubtracted dispersion relations) not available in any other process.

To illustrate the value of higher energy photon beams, a few examples of interesting experiments to do are listed below:

1. The total photon cross sections on protons and neutrons have been observed to approach each other and both to approach a constant asymptotic value. This situation is similar to our knowledge of meson total cross sections before the Serpukhov measurements were made. It is of great interest to extend the energy range of these experiments and to study coupling to Regge trajectories as well as vector dominance models.
2. Compton scattering experiments also test the Regge hypothesis for the couplings to the nucleon and the photon as well as vector dominance. Present experiments at energies up to 18 GeV indicate some disagreement with current models. The real part of the Compton scattering amplitude can be measured via Bethe-Heitler interference measurements. All these experiments will profit greatly from higher energies.

3. Pseudoscalar meson photoproduction experiments have indicated a great deal of regularity in the energy and momentum transfer dependences of the cross sections. These regularities are obtained in some theoretical models by balancing many terms with different dependences to get the relatively simple energy and momentum transfer dependence observed. This balancing act cannot be done presently over a greatly expanded energy region, and hence it is important to extend these studies to higher energies, and especially important to do them with polarized photons.

4. Observed vector meson production cross sections decrease slowly if at all with incident energies. Measurements of these cross sections at higher energies and in nuclei provide a crucial test of models such as vector dominance.

5. The search for new vector mesons by their diffraction production and for other natural spin-parity mesons (Regge recurrences) initiated by photons can be extended. This is complementary to similar searches using pion or kaon beams which diffraction-produce unnatural spin-parity mesons. The reaction $\gamma + p \longrightarrow V + N^*$ with detection of the vector meson can similarly be used to study baryon resonances.

6. S-channel helicity conservation in vector meson photoproduction can be tested out to large values of $|t|$. Very little is known about this in the case of mesons because at the lower energies one-particle exchange seems to still play an important role. As mentioned before, it would be of great importance to see how far in $|t|$ this rule applies to ρ^0's. If the present $|t|$ dependence is maintained, exploration out to $|t| - 2(\mathrm{GeV}/c)^2$ can be carried out.

Hadron Physics:

The RLA will also be a copious and effective source of secondary hadron beams as shown in Table II. While the improved duty cycle will allow some experiments with pion beams which cannot be done now, the greatest interest will lie in the 25-45 GeV region. This is beyond the reach of the CERN-PS and the BNL-AGS proton synchrotrons. Also, the variety of experiments will be enhanced over the present ones by the introduction of useful K^-, $\bar{p}$ and $\bar{n}$ beams. The neutral K^0 and $\bar{n}$ beams at SLAC are exceptionally clean compared to those at NAL, being relatively free of neutron backgrounds. Reasonable momentum measurements of these neutrals can be made up to energies of 7 GeV by time-of-flight methods based on the intrinsically short rf bunches (10^{-11} sec) in the SLAC pulse.

The interest in hadron beams in the high energy region is that they will provide present knowledge of the energy dependence of specific processes, the isolation of diffractive from exchange processes, the search for new diffractively produced resonances, the search for exotic exchanges, the search for heavy mesons, etc. Current theoretical ideas of duality, factorization, etc., have predictions in this energy range which will be tested. SLAC's experiments would serve as a very important supplement to the hadron physics at NAL.

The yields given in Table II are for secondary momenta of 10-40 GeV. These yields are lower than NAL's (by a factor of 10-100 for 5×10^{12} protons/sec). However, for reasonable cross sections where fluxes exceed or match the capacity of data handling systems, SLAC will be a valuable complementary facility to NAL — as it now serves to Brookhaven and CERN.

For processes having reasonable cross sections, wire chamber spectrometers with huge event rate capabilities and reasonable acceptances for high mass resonances can be used quite profitably at SLAC. The large aperture solenoid system

now being built at SLAC, can be used at these higher energies without extensive modification.

Bubble Chamber Physics:

SLAC has unique characteristics with respect to bubble chambers, namely:

a) High repetition rate

b) Characteristically short pulses

c) Internal phase bunching

d) Pulse-by-pulse beam switching

They have all led to a very productive program of high statistics experiments, mostly in hadron physics, but also to a significant series of investigations into photoproduction.

In addition, a number of unique applications, developed at SLAC, have broadened the scope of the bubble chamber technique. Thus, for practical purposes, the physics proposed at SLAC at the higher energies will not be attainable at other laboratories. These are:

a) Time-of-flight measurements of the momentum of neutral kaons and neutrons (extendable to antineutrons at the higher energies) by counters surrounding the chamber.

b) Fast cycling (10-20 pps) of large (1-2 m long) hydrogen chambers; the lights are flashed only when a very fast forward particle is observed and its momentum is measured by spark chambers placed behind the bubble chamber.

c) Rapid cycling chambers of target size (45-90 pulses per second and 30-60 cm long) with thin beam windows all around. When the lights are triggered by counter-spark chamber arrays, the chamber becomes a visible hydrogen or deuterium target.

An important feature of these techniques is that, because the chamber has 4π geometry, many biases can be turned off for part of the experiment by running in an untriggered mode. A second feature, peculiar to SLAC, is that when the proposed system operates at 20-50 GeV, the number of beam particles per pulse acceptable to a bubble chamber (15-20) exceeds that acceptable to a spark chamber (5-10); thus the bubble chamber as a target is more than matched to its counter spark chamber system. As would be expected, most of the benefits to bubble chamber physics from this proposal will accrue at the higher energies.

Keeping these points in mind, one can see that there exist a large class of experiments in the 20-50 GeV range that can be done at SLAC in a highly competitive and perhaps unique manner. Among these are:

a) Studies of energy dependence and differential cross sections for highly peripheral quasi two-body reactions involving backward nucleon resonances. These are excellent experiments for the fast cycling chambers; one such experiment has already been completed at 14 GeV using the SLAC 40 in. chamber.

b) Studies similar to (a) except where the final state involves a backward hyperon resonance. These are particularly suited to the rapid cycling target chamber because of the short life-time involved.

c) Studies of nucleon-antinucleon resonances such as $R^+ \longrightarrow \bar{n}p$ by triggering on a fast forward $\bar{n}$ in a reaction $\pi^+ p \longrightarrow \bar{n}pp$.

d) Studies of antilambda proton elastic scattering by triggering on fast forward protons in $K^+X \longrightarrow \bar{\Lambda}X'p$ and observing the $\bar{\Lambda}p$ scattering in the chamber.

e) Studies of exotic exchanges by triggering on fast forward nucleons and looking in the chamber at backward produced mesons. These studies would be especially unique for backward going K^O's.

Conventional use of a 2-3 meter chamber (with good optics and high resolution) will still be available, with its small demand (1-2%) on machine intensity, for studies of high mass resonances and multiple particle final states. Neon-hydrogen mixtures will extend these to states with several neutral π's. A chamber of this size with a field of 25-30 kG is quite capable of the resolution needed.

Conclusion:

To summarize this section of the report, there is a large, quite unique and fundamentally important class of high energy physics experiments which would constitute the exclusive territory of the Recirculating Linear Accelerator: these are the investigation of the structure of the nucleon at very high momentum transfers and the study of strong interactions by means of the polarized photon. In addition, a large, competitive and quite fruitful series of experiments in hadron and weak interaction physics would further enhance the general desirability of achieving the objectives of this proposal.

ADDENDUM TO SECTION II

Since the RLA description and physics program (Section II above) was written, approximately seven months ago, several new experimental techniques have been proved out at SLAC which would lead to an even more interesting use of the RLA, especially at the higher energies, than was described in Section II. The purpose of this addendum is briefly to describe these techniques and the consequent experiments and to amplify on the role of wire chamber spectrometers in studying lepton and photon interactions. There is also a comparison of single arm spectrometer inelastic electron scattering event rates in the two versions of RLA vis-a-vis in a similar experiment using muons at the National Accelerator Laboratory. In addition, there is included a theoretical remark on the importance of wide angle Compton scattering.

Superconducting Tube to Reduce Bethe-Heitler Background

The use of such a tube to create a field free region for non-interacting beam particles has been under investigation at CERN and SLAC for more than a year. Such a tube is particularly needed at a poor duty cycle electron accelerator because the most severe limitation on the useful number of electrons or photons per pulse into a large solid angle device is the e^+e^- background. Because of the inherently small production angle for the pairs, this background (in a field free region) travels undeflected along with the beam. The hadrons, produced at larger angles escape into the region of the field and are bent into a detector.

An experiment detecting electroproduction of ρ^0 mesons at fairly large q^2 values has had a successful checkout run at SLAC where, using very large optical spark chambers as detectors, a flux of 5×10^4 e^-/pulse [$\sim 10^7 e^-$/sec] was achieved. In this case the tube was placed in a field of 15 kG and the field inside the tube was less than 50 gauss. The success of this method depends very much on a very tight electron beam (spot size of $\sim 2 \times 2$ mm) and angles of $\sim 10^{-6}$ radians. This technique can easily be used in experiments at the highest RLA energies.

Monochromatic-Polarized High Intensity Photon Beams Using Diamond Radiators

Recently an rf sputtering technique has been successfully used at SLAC to thin diamond crystals at the rate of 1 mil/day. Using this technique one expects to get 3-4 mil pieces. With collimation one can achieve 45% polarization and

have ~50% of the photons inside a $\Delta E/E$ of $\pm 2\%$ for intensities of 10^7 photons per pulse (2×10^9/sec) at a photon energy equal to 3/4 of the incident electron.

Using the superconducting tube technique mentioned above this beam can be used in the same way as the electron beam with roughly the same intensity. In addition, it can be used at full intensity with single arm spectrometers as was briefly mentioned in Section II.

Well-Defined μ Beams

Two new μ beams have recently been developed at SLAC in connection with proposed μ-p inelastic experiments using triggered bubble and streamer chambers as detectors. The μ beam for the bubble chamber has been completed and tested with the following results:

Energy	~16.5 GeV/c
Momentum spread	±2% [only 0.02% lie outside this bite]
Intensity	100 μ/pulse for E_ℓ = 19.5 GeV
Size (matched to B.C.)	1"×8"
Halo	2% of the particles lie outside the 1"×8" beam
π/μ ratio	10^{-6}

With this beam it has proved quite easy to separate single π^0 or neutron from multiple neutral events.

The experimental-possibilities of these techniques are:

A. Lepton and Photon Interactions Using Wire Chamber Spectrometer

The LASS spectrometer, under construction at SLAC, can, when coupled with the superconducting tube, now be considered as an important future tool in the study of lepton and photon interactions. Using the fluxes quoted above the following typical rates are expected:

(1) Photoproduction

Experience with superconducting tubes, plus the trapping effect of the solenoidal field in LASS, indicates that 2000 q per pulse can be run through a 1-m liquid hydrogen target for the poor duty cycle conditions and about 100 times more for the good duty cycle configuration.

These assumptions lead immediately to the following event rates:

20 GeV, good duty cycle	100 events/sec/μb cross section
40 GeV, poor duty cycle	1 event/sec/μb cross section

Typical event rates would then be:

(a) Study of rho photoproduction on H_2
($\sigma \sim 10\,\mu$b)

$$\frac{3.6\times10^{6} \text{ rho events/hr at 20 GeV}}{3.6\times10^{4} \text{ rho events/hr at 40 GeV}}$$

(b) Inelastic Reaction Channel (single process)
($\sigma \sim 0.02\,\mu$b at 20 GeV, $0.005\,\mu$b at 40 GeV)

$$\frac{700 \text{ events/hr at 20 GeV}}{2 \text{ events/hr at 40 GeV}}$$

These rates can be obtained with polarized or unpolarized photon beams and are sufficient for very detailed and systematic study of the s- and t-dependence of photoprocesses in the 10-20 GeV range.

The rates in the 40 GeV region are such that present-day-type experiments will be accomplished with modest amounts of machine time (e.g., 100 hours).

(2) Inelastic Electron Scattering

Again from experience with the superconducting tube 2×10^{4} e^{-} per pulse in poor duty cycle conditions and about 100 times more in the good duty cycle mode can be used. Using this flux figure and reasonable estimates of the deep inelastic electron scattering cross section, the following counting rates may be obtained.

Table A

Counting Rates per hour at $q^2 = 2, 4$ GeV^2 and
$W \geq 2, 3, 4$ GeV in intervals of $\Delta q^2 = 0.1$

	20 GeV (good duty cycle)			40 GeV (poor duty cycle)		
	$W \geq$ (GeV) 2	3	4	2	3	4
q^2=2 GeV^2	4100	3400	1600	70	40	50
q^2=4 GeV^2	800	510	250	20	15	10

Table B

Counting Rates per hour for various cuts in q^2, W variables

	E_e = 20 GeV (good duty cycle)		
$W \geq$	2 GeV	3 GeV	4 GeV
	($\times 10^3$/hr.)	($\times 10^3$/hr.)	($\times 10^3$/hr.)
$q^2 > 0.5$ GeV^2	390	230	110
$q^2 > 1.0$ GeV^2	160	100	50
$q^2 > 1.5$ GeV^2	85	55	30
$q^2 > 2.0$ GeV^2	40	35	15
$q^2 > 2.5$ GeV^2	30	25	12
$q^2 > 3.0$ GeV^2	20	15	10
$q^2 > 4.0$ GeV^2	10	10	5
	E_e = 40 GeV (poor duty cycle)		
$q^2 > 0.5$ GeV^2	6	4.5	3.0
$q^2 > 1.0$ GeV^2	3	2.2	1.5
$q^2 > 1.5$ GeV^2	1.5	1.3	0.9
$q^2 > 2.0$ GeV^2	1.0	0.9	0.6
$q^2 > 2.5$ GeV^2	0.7	0.6	0.4
$q^2 > 3.0$ GeV^2	0.5	0.4	0.3
$q^2 > 4.0$ GeV^2	0.2	0.3	0.2

B. μ p Scattering Using Track Chamber Techniques

Actual results achieved in an ongoing experiment at SLAC, using the 1 meter chamber operating at 8.5 pulses per second, where the chamber lights were triggered by external counters, can be extrapolated to a 40 GeV μ beam into a 3.5 meter chamber operating at 10 expansions/second and 200 μ's/pulse with the following rates:

For $W \geq 2$ (mass of virtual photon)

q^2 >	Rate/hour
0.5	42
1.0	20
1.5	10
2.0	3.0
2.5	4.0

or ~2000 events/day for $q^2 > 0.5$ $W \geq 2$ (deep inelastic). These experiments can also be done in deuterium and, if interesting, in neon. Using a streamer chamber one could expect rates 5 - 10 times as great.

The superconducting tube technique may also be considered for a hydrogen bubble chamber where as many as 10^5 electrons per pulse could be contemplated in which case one inelastic event would be produced every 3 - 5 expansions, or a rate of 50-60,000 events per day.

Comparison Counting Rates for Single Arm Inelastic Electron Scattering in a SLAC Spectrometer with an NAL Single Arm Muon Scattering Experiment

It is interesting to compare these counting rates because they show that, even though the NAL experiments encompass values of the kinematic variables beyond the reach of RLA, the range of useful rates makes the effective range of these variables greater for RLA. In Fig. A the ep single arm results are shown for the 20 GeV incident electron case, and in Fig. B for the 50 GeV case. These tables cut off at 200 events/hour, which from experience at SLAC is what is needed in order to make radiative and other corrections.

The muon events shown in Fig. C are cut off at 10 events per hour, on the assumption that an order of magnitude less counting rate is tolerable both because it is a good duty cycle machine and because the particles are muons

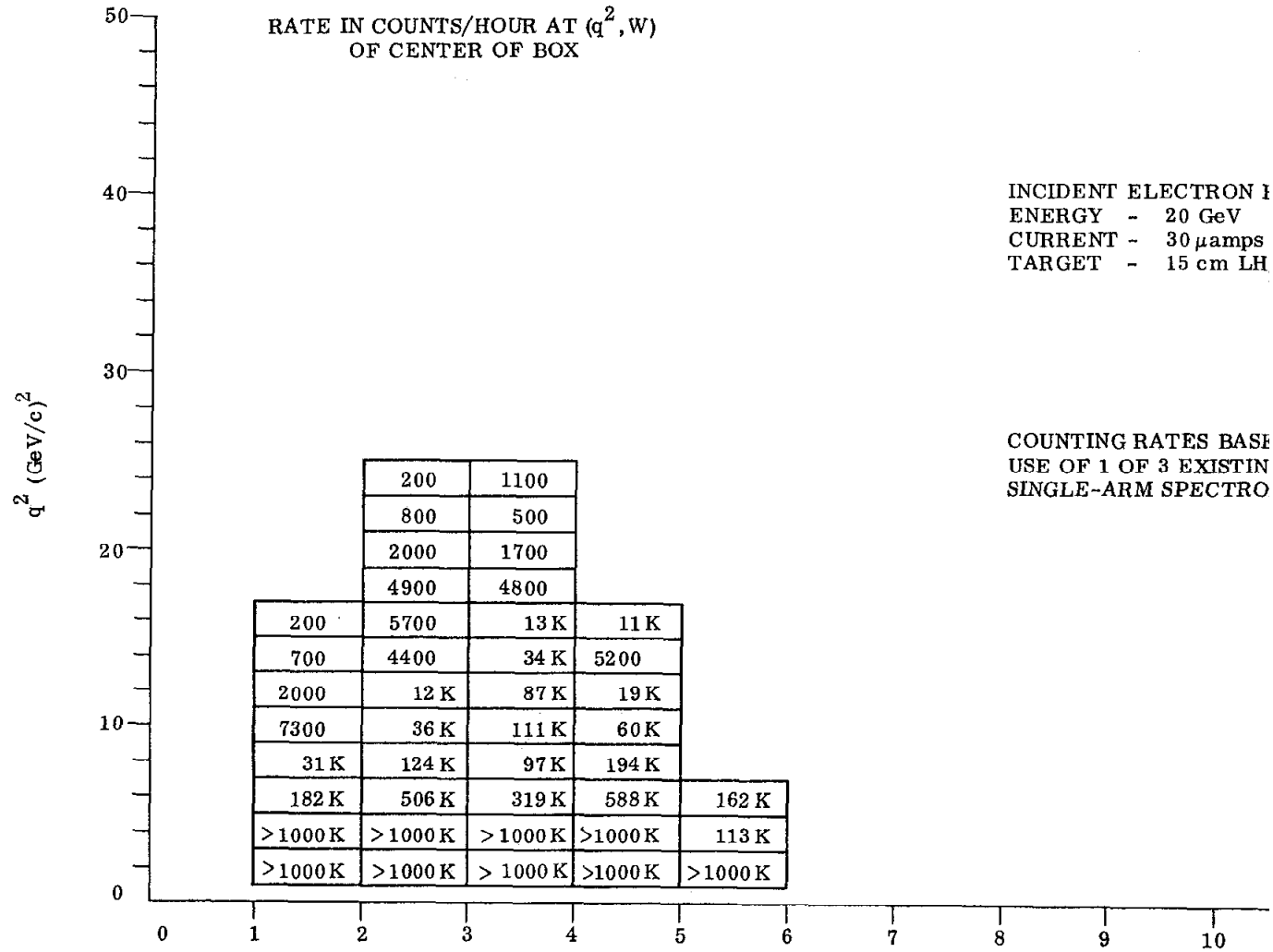
RATE IN COUNTS/HOUR AT (q^2, W)
OF CENTER OF BOX
INCIDENT ELECTRON I
ENERGY - 20 GeV
CURRENT - 30 μamps
TARGET - 15 cm LH
COUNTING RATES BASI
USE OF 1 OF 3 EXISTIN
SINGLE-ARM SPECTRO
q^2 (GeV/c)^2
W, FINAL-STATE HADRON MASS (GeV)
0
10
20
30
40
50
1
2
3
4
5
6
7
8
9
10
200 1100
800 500
2000 1700
4900 4800
200 5700 13 K 11 K
700 4400 34 K 5200
2000 12 K 87 K 19 K
7300 36 K 111 K 60 K
31 K 124 K 97 K 194 K
182 K 506 K 319 K 588 K 162 K
>1000 K >1000 K >1000 K >1000 K 113 K
>1000 K >1000 K > 1000 K >1000 K >1000 K

FIG. A

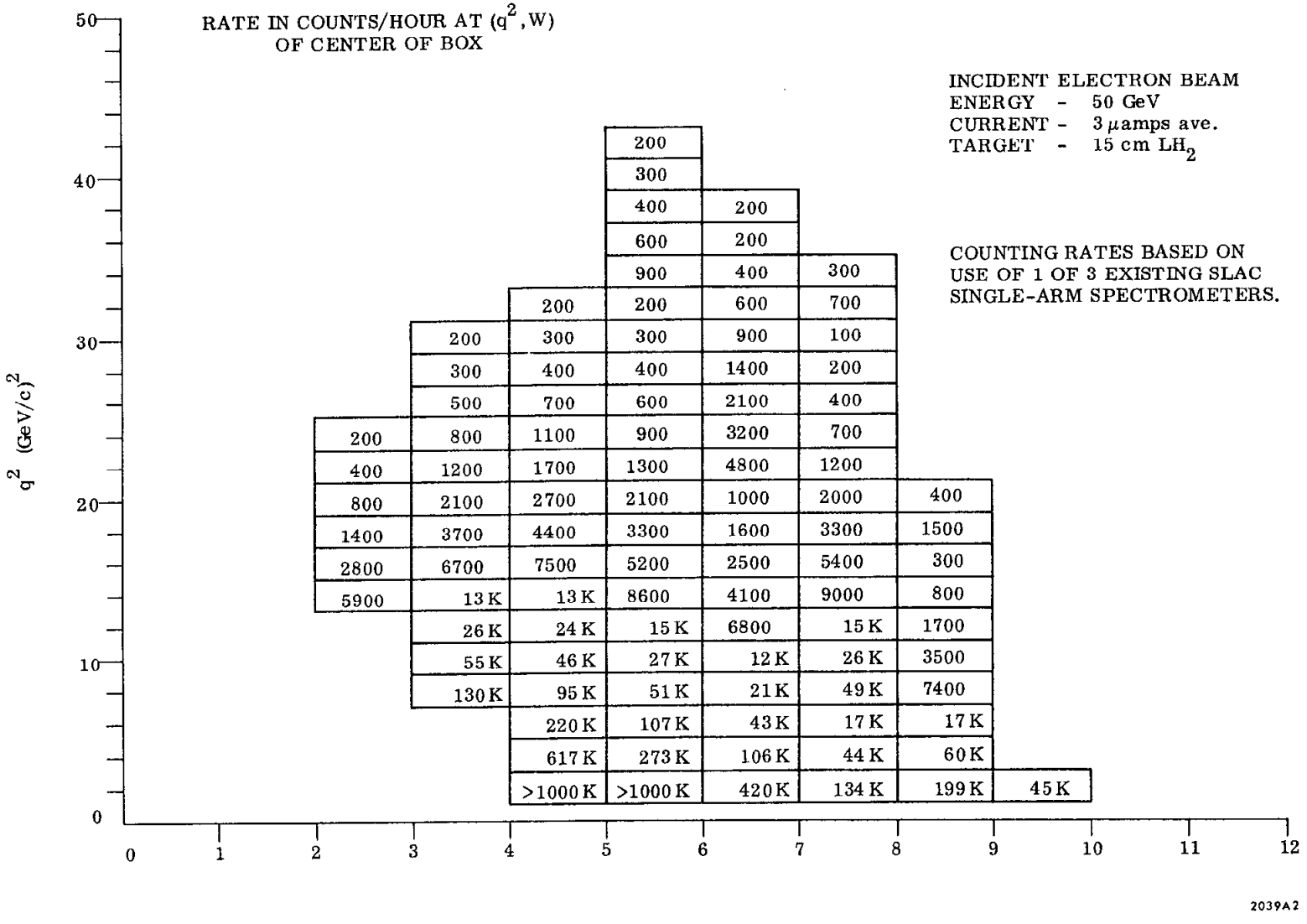

q^2 \ W	0	1	2	3	4	5	6	7	8	9	10	11	12
50						200							
40						300							
						400	200						
						600	200						
						900	400	300					
					200	200	600	700					
				200	300	300	900	100					
				300	400	400	1400	200					
				500	700	600	2100	400					
			200	800	1100	900	3200	700					
			400	1200	1700	1300	4800	1200					
30			800	2100	2700	2100	1000	2000	400				
			1400	3700	4400	3300	1600	3300	1500				
			2800	6700	7500	5200	2500	5400	300				
			5900	13 K	13 K	8600	4100	9000	800				
				26 K	24 K	15 K	6800	15 K	1700				
20				55 K	46 K	27 K	12 K	26 K	3500				
				130 K	95 K	51 K	21 K	49 K	7400				
					220 K	107 K	43 K	17 K	17 K				
					617 K	273 K	106 K	44 K	60 K				
10					>1000 K	>1000 K	420 K	134 K	199 K	45 K			
0													

FIG. B

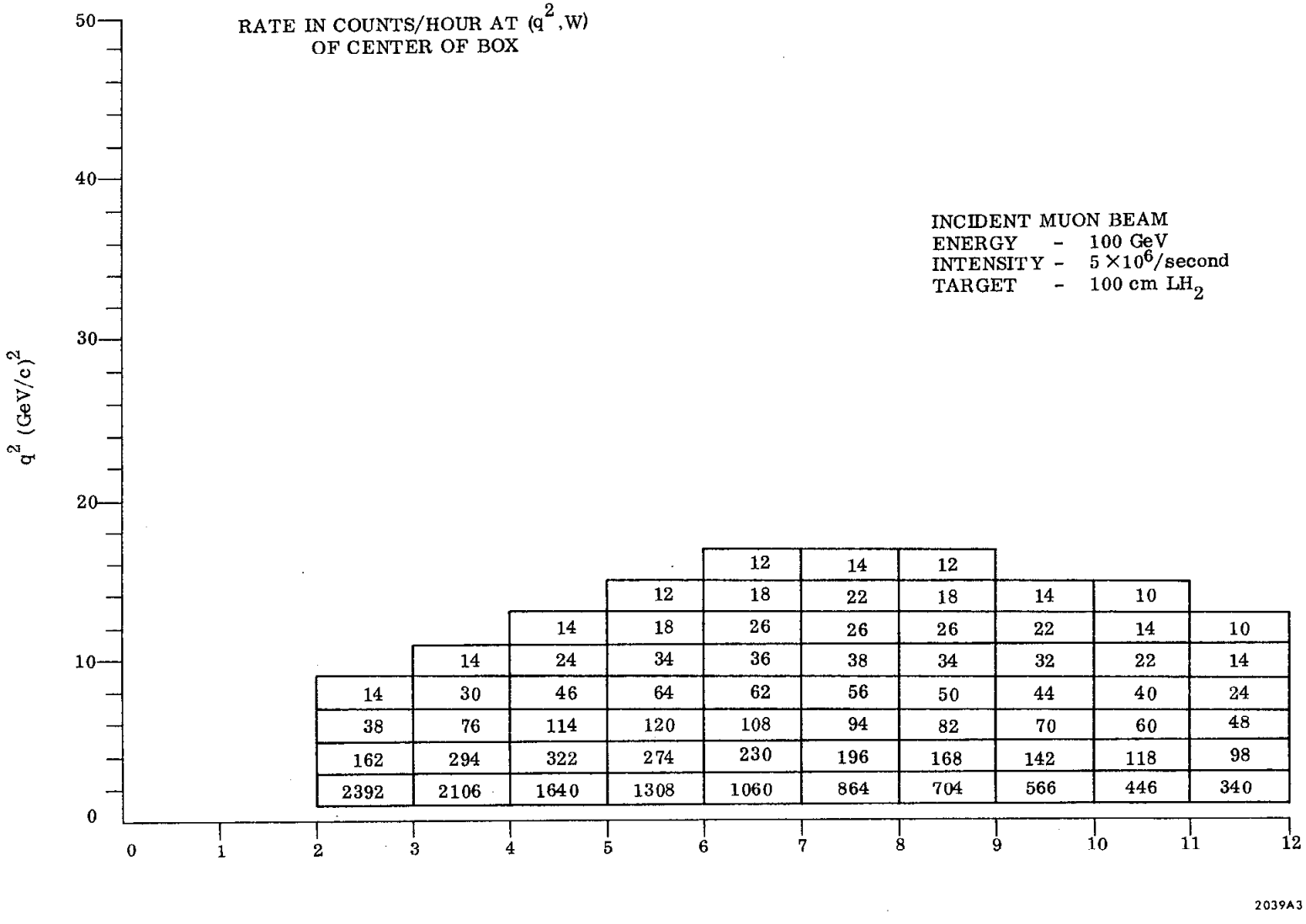

W, FINAL-STATE HADRON MASS (GeV)

FIG. C

rather than electrons. The result is that the only place where the NAL muon experiments become competitive with SLAC is for low q^2 and very large hadron mass states. For all other values the RLA rates are many orders of magnitude greater.

Hadron Physics

There are several experiments of a programmatic nature which require long running times, but are nevertheless important. From past experience at proton machines not many of these are completed per year and SLAC could make significant contributions in this field. Examples are: polarization parameters in πp and Kp elastic scattering; detailed examination of multineutral final states; and low cross section states in πp and Kp interactions in the 5-10 GeV region. Examples of the latter as would be measured by LASS are backward processes, exotic exchanges and large t processes. The good duty cycle will allow $\sim 2 \times 10^5$ π/sec intensities to be used so that backward $\pi p \rightarrow px$ which have 1 μb cross sections will yield 2500 eV/hour while large t events in the same process having cross sections between 0.01 - 0.1 μb will still give 25 - 250 eV/hour/GeV^2.

The Compton Amplitude

The complete Compton amplitude of the nucleon is basic in the study of the electromagnetic properties and structure of the hadrons. Compton scattering and Bethe-Heitler interference measurements may be one of the most sensitive areas for tests of parton models, current commutator theories, and other theoretical ideas which account for scaling in electron-proton inelastic scattering. The extended capabilities of RLA in duty cycle and higher energy are essential for performing many of these tests. For example:

(1) Bethe-Heitler interference experiments (electron-positron wide angle bremsstrahlung or asymmetric pair production on a proton target) give direct measurements of the interfering real part of the Compton amplitude with one virtual proton. Extrapolated to photon mass $q^2 = 0$ and $t = 0$, this supplies a fundamental test of the Kramers-Kronig (Gell-Mann,Goldberger) dispersion relation. A critical question will be the confirmation of the constant real term in the high energy forward amplitude (as conjectured by Drell, Creutz, and Paschos, and analyzed from $\sigma_{\gamma p}$ data by Gilman and Damashek).

(2) Recently it has been found that the existence of the above "J = 0 fixed pole" term in the forward Compton amplitude is a necessary consequence of parton models and gauge-invariance (Brodsky, Close, Gunion). The behavior of this real energy-independent term in the complete Compton amplitude is rather surprising: For fixed t, it is independent of either photon mass; its t-dependence is similar to the Dirac proton form factor $F_1(t)$. These predictions of a parton model can be tested rather cleanly by wide angle bremsstrahlung measurements, which should be possible with the improved duty cycle of RLA.

(3) Parton theories also account for a breakdown of vector dominance relations connecting ρ-photoproduction and Compton scattering in both normalization and t-dependence. In particular, the Compton amplitude is predicted to fall slower in t than the rho photoproduction amplitude due to the presence of the fixed pole term (with dipole dependence) in the two photon amplitude. Also, the photon polarization is predicted to satisfy spin conservation rather than s-channel helicity conservation at large t. Higher SLAC energy will be important for clear tests of these parton ideas. Finally, on purely experimental grounds, Compton scattering is a very important process to measure independent of any models.

III. GENERAL DESCRIPTION OF THE RLA

A. Functional Concept

The project described in this report will boost the energy of the SLAC two-mile accelerator to the 40 GeV range. This energy increase will be achieved by recirculating the electron beam to accelerate it through the accelerator twice instead of only once as at present. The proposed system also makes it possible to produce beams up to 17.5 GeV (initially) with duty cycles 100 times as high as presently attainable.

The implementation of this proposal involves the acceleration of a beam through the two-mile accelerator to an energy of 17.5 GeV followed by storage of the beam for approximately 122 revolutions around a 6900 meter storage path (see Fig. 7). The storage path consists of two transport lines carrying the beam in opposite directions through two tubes parallel to the accelerator inside the accelerator housing. The direction of the beam is reversed in magnet loops located at the ends of the accelerator. Beam storage is limited initially to 17.5 GeV to keep the synchrotron radiation energy loss in the loops (which varies as the fourth power of the energy) to a reasonable value. During each revolution in the storage system, a 17.5 GeV beam loses a total of 125 MeV due to synchrotron radiation. This energy is restored by means of two conventional 333 ft. accelerator sectors. The gradient in these sectors is high enough to result in an energy gain of 125 MeV while permitting off-crest positioning of the beam for synchrotron phase stabilization purposes. The design of the recirculation loop and the magnets will permit later increase of the storage energy to a maximum of 25 GeV. Increasing the energy of the stored beam to 21 GeV can be accomplished by doubling the length and power of the rf system (from two to four 333 ft. sectors). Increasing the stored energy to 25 GeV appears to be economically feasible only by the use of superconducting

accelerator sections. The development of such superconducting structures is now underway at several laboratories.

The recirculating period is about 23 microseconds. The number of revolutions is adjusted so that the total storage time, 2.8 milliseconds, is equal to the normal interpulse time interval of the accelerator when it is operating at 360 pulses per second. At the end of this storage interval, the beam is reinjected into the accelerator and is accelerated a second time, gaining 25 GeV (when conversion of the present 20 MW klystrons to 30 MW models is completed) resulting in a final energy as high as 42.5 GeV. Other modes of operation are also feasible as discussed later.

The main bend rings contain an array of alternating-gradient magnets. To adapt to the configuration of the SLAC site, the bending radius of the rings has been limited to 95 meters. By reducing the gaps between magnets to the practical minimum, the resulting radius in the magnets is 88 meters. The sum total of all the bends around the loop is 480°.

At the west (injector) end of the accelerator, the recirculating loop will be located almost on the surface of the existing grade. At the east (research) end, the recirculating beam passes through the wall of the accelerator housing beyond Sector 30. Thus, the beam will be recirculated through the entire length of the accelerator housing. This results in the maximum increase in energy while minimizing modification of the existing facility.

The ultimate energy which can be reached increases as the single-pass accelerator energy becomes greater. In this discussion, it is assumed that during the next few years the accelerator energy will be increased gradually from the present maximum ($\sim$ 22 GeV) to a higher level (25 GeV) by conventional means, i.e., increasing the rf input power to the accelerator by installing 30 MW klystrons.

Even higher power (60 MW) klystrons are under development; with a full complement of such tubes, the single-pass accelerator energy would be 35 GeV and the maximum output beam energy using the recirculation technique would become 60 GeV (assuming that the storage energy has been increased to 25 GeV).

Modes of Operation:

Various modes of operation will be possible with the RLA. The modes differ with respect to maximum beam energy, beam current, repetition rate and duty cycle (values of which are given in Table I). A brief discussion of these various ways of operating follows:

1. High Energy Mode (25-42.5 GeV)

After accelerating to 17.5 GeV (initial maximum) energy, the beam is stored for 2.8 milliseconds in the recirculating loop. The beam is then reinjected into the accelerator for a second acceleration passage which increases the energy by 25 GeV (maximum). The final energy is then 42.5 GeV. To operate at full 360 pps rate, a new beam pulse is injected into the accelerator at the same time as the stored beam is injected for the second passage. Both the high and low energy beams are accelerated at the same time. To allow the energy gains during the first and second passages through the accelerator to be different, say 17.5 and 25 GeV respectively, while retaining the full 360 pps capability, an off-axis injector will be provided. This injector will be located along the accelerator at a position determined by the ratio of the energy gains of the first and second accelerating passages. In the beam switchyard the two beams are separated by magnets. The amount of rf power and accelerator length initially provided in the loop is based upon storage of a 10 mA beam at an energy of 17.5 GeV. At lower recirculating energy, the recirculating current can be increased until beam loading in the loop accelerator system begins to affect beam stability. Depending on the final design

parameters of the accelerating structure, this limit will probably be about 25 mA. As discussed above, the recirculation system is expandable to an energy of 25 GeV and the accelerator energy can be increased to 35 GeV by the future installation of 60 MW klystrons. Thus, the maximum energy of the high energy mode could later be increased to 60 GeV.

2. High Duty Cycle Mode (17.5 GeV Maximum)

The present accelerator beam has a duty cycle of $\sim 6 \times 10^{-4}$. By slowly "peeling off" a portion of the stored beam during each transit around the loop, the recirculating scheme described above can provide a duty cycle two orders of magnitude higher ($\sim$ 7%) at energy levels up to 17.5 GeV. This increased duty cycle is the ratio of pulse length (1.6 microseconds) to the recirculating period (23 microseconds). Assuming 10 mA circulating beam current and 360 pps, the average output beam power in this operating mode is $\sim$ 100 kW. As described above, the recirculating current can be significantly higher at a lower value of the storage energy. The recirculation energy is expandable to 25 GeV as noted previously.

3. Accelerator Only Mode (25 GeV Maximum)

This mode is essentially identical to the present way in which the accelerator is operated except that the beam energy (up to $\sim$ 25 GeV maximum) is higher as a result of increasing the rf power output at each klystron station to 30 MW. The maximum beam current will be as high as presently achievable ($\sim$ 82 mA) or even slightly higher. By later replacing the 30 MW klystrons with 60 MW models, the accelerator energy could be increased to 35 GeV. The repetition rate of the higher power tubes would be reduced to 180 pulses per second to keep the total power requirements within reasonable limits.

B. General Layout

A general layout of the entire recirculation system is given in Fig. 7. The beam is extracted from the end of the accelerator, upstream of the present collimators and pulsed magnet system, and inflected into the recirculator. The east-end loop starts out with a 12° bend to extract the beam from the accelerator housing. Following this bend, the trajectory consists of a 198° circular loop with a 95 m radius. The beam then goes through a straight section followed by a 30° reverse bend. Reentry into the housing takes place at Sector 26.

Following the beam direction, the west-end loop takes off from the accelerator housing at Sector 4 and reenters it upstream of the injector. It consists of a 30° reverse bend, a long straight section and a 210° circular bend, also with 95 m radius. In order to conform to the local terrain, the plane of this loop is tilted down towards the south at 4% grade. Reinsertion is accomplished by a fast pulsed magnet which is only activated on the last pass through the recirculator.

The rf system which supplies the energy lost by synchrotron radiation in the loops is located in Sectors 21 and 22. It consists of two regular sectors of SLAC accelerator powered by sixteen 220 kW klystrons operating at ~ 10% duty cycle. This initial system is capable of supplying up to 150 MeV per turn. At a later date, it may be possible to increase this energy, either by adding more conventional sections or by installing some superconducting sections operating CW. With a standing-wave gradient of, for example, 6 MV/m in a 13 m long superconducting structure, the beam would gain up to 75 MeV per pass. By having the beam traverse the structure in both directions, the total energy gained in each cycle could be as high as 150 MeV.

High duty cycle beams at the recirculator energy are extracted by a septum magnet system which "spills" some of the electrons into the beam switchyard by

"peeling off" a fraction of the beam on each turn. When operating in the energy doubling mode, this system is turned off and the beam proceeds around the loop 122 times. On the last turn, the pulsed magnet at the injector is turned on and the beam is reinserted into the two-mile accelerator for a second pass.

The beam dynamics in the RLA are described in detail in Section IV. Only a brief functional description is included here. Assume an electron beam with energy E (between 12 and 17.5 GeV) emerging from the accelerator and being inserted into the recirculating system. Suppose that this beam consists of a 1.6 μsec pulse train of $\sim 5^{\circ}$ bunches ($\sim$ 1.5 mm long) with energy spectrum $E/E_0 = \pm 0.2\%$. As these bunches are bent by 210° in the east-end loop, the characteristics of the magnetic transport system cause them to grow to a length of about 6 mm. This happens because the bend is not entirely isochronous; thus the high energy electrons have a longer trajectory than the ones with the exact energy E_0. The function of the 30° reverse bend is to return the beam to the accelerator housing and to restore the bunch to approximately its original length. This feature is achieved by dispersing the beam in momentum with a set of bending magnets. Following this dispersion, there is a quadrupole doublet which causes the high momentum rays to cross over and enter a second bending system. Because of this cross over, the trajectory of the higher momentum electrons can be made shorter than that of the equilibrium orbit in the second bending system. Thus, when the bunches reenter the accelerator housing, quasi-isochronism is reestablished. The degree of quasi-isochronism is adjustable. It determines the momentum compaction of the loop and the period of synchrotron phase oscillations. As the beam goes through the straight sections parallel to the accelerator, a periodic focusing system keeps its cross section within acceptable bounds. In the west-end loop, the steps just described for the east-end loop are now reversed.

It is essential that the six-dimensional phase space of the bunches as they go through the recirculator be controlled in such a way that the beam can be reinserted into the accelerator. In particular the bunch length must stay within 10-20^{o} in order to keep the energy spread after the second acceleration within acceptable limits. Details of these problems including damping, beam loading, tolerances and instabilities are discussed in the section on beam dynamics.

C. Components and Facilities

1. Magnets and Power Supplies

The magnets for the recirculating system can be divided into several categories:

a. Alternating-gradient 3^{o} bending magnets for the circular loop arcs (65 magnets for the east-end loop and 69 magnets for the west-end loop). Each cell will consist of a focusing magnet with index n = -900 and a defocusing magnet with index n = +700. Each magnet will have a mean field of 6.58 kG at 17.5 GeV. A total of 11 power supplies will be available, one power supply powering an average of 12 to 14 magnets. The power supplies will be of the conventional silicon controlled rectifier type. Since the beam loses energy around the loop, successive power supplies will run at slightly decreasing values of current. The question of whether a separated function lattice would be superior has been discussed at some length. Tolerances would probably be easier to meet in such a system but the radius of the loops would have to be increased to accommodate the extra quadrupoles. The limitations of available real estate and tunnel construction costs make this solution less appealing.

Four magnets of similar design but with zero-gradient will be used in the 12^{o} bend.

b. Zero-gradient 2.5^{o} bending magnets for the 30^{o} reverse bends. There will be 12 such magnets in each bend. The first three of each group are the energy dispersing magnets, the last three are the energy recombining ones; the middle six are

those which cause high energy electrons to have a shorter path length. One power supply will be used per loop.

c. Zero-gradient 1.5^{o} bending magnets for η-function matching between the circular loops and the straight sections. There will be 4 such magnets, each powered by one power supply.

d. Each of the above 1.5^{o} zero-gradient magnets will be accompanied by a quadrupole singlet, each supplied by its own power supply. Two doublets using identical quadrupoles will be used in the 12^{o} inflection system.

e. As described earlier, each reverse bend will contain two sets of doublets for a total of 8 quadrupoles and 8 power supplies. Sixteen very similar quadrupoles will be used for phase space matching along the long straight sections in the loops, each with its individual power supply.

f. The long straight sections parallel to the accelerator will use 66 quadrupoles. For ~100 m long sectors, this will mean one quadrupole per sector. Each quadrupole will have its individual power supply. Two of the same quadrupoles will be used as symmetry quads in the reverse bends.

g. In addition, there will be a number of special magnets, some to extract the beam from the accelerator and to inflect it into the recirculator, some to reinsert it into the accelerator, some for the "long spill," and some to upgrade the existing switchyard. Some of the inflection and reinsertion magnets will have to be pulsable with 2 μsec flat top and less than 21 μsec total rise and fall time so that the magnetic field is off when the beam returns after traveling around the loop (~23 μsec). The power supplies for these magnets will be line-type pulsers. In addition, there will also be a number of small steering magnets.

2. Tunnels, Buildings and Roads

As shown in Fig. 8, the beam transport components will be installed in underground cylindrical pipes (precast concrete storm drains). Additional concrete will be poured into the bottom of the pipes to create a flat surface for easier movement of personnel and small vehicles. Joints at the ends of the pipes will be tongue-and-groove and will be sealed to keep out ground water. The pipes will be 8 ft. in diameter (I. D.) and 8 ft. long. This diameter is large enough to house the magnets and other beam components and still allow room for passage of personnel.

Each loop will contain 3 equipment penetrations (8 ft. in diameter) and 3 man accessways (3 ft. in diameter). These penetrations will be offset from the beam centerline in order to minimize the radiation escaping from the tunnel.

The only special buildings required are 5 small (16 ft. × 32 ft.) structures located at each end of the recirculator to house the dc power supplies.

An access roadway 14 ft. in width will be constructed along the east and west end loops. This will allow two-way traffic for service vehicles. The general layout of the plant is shown in Figs. 9, 10, and 11.

3. Support and Alignment

Supports must be provided for the magnets in the bends at the ends of the recirculator and for the beam transport pipes and accelerator sections in the accelerator housing. Other devices such as beam monitors, collimators and steering dipoles must also be supported at various positions in the loop. The problem of supporting magnets, etc., in the bends is complicated by the fact that the plane of the west-end loop is tilted with respect to the horizontal plane by a 4% slope.

The beam transport pipes in the Accelerator Housing will be 2-1/4" OD stainless steel tubes. The pipe transporting the eastbound beam will be located 29 in. above the present accelerator centerline (see Fig. 12). The second pipe, which

transports the westbound beam, will be at the same elevation but 24" farther to the south. Both pipes will be attached to the present 40 ft. support girders of the accelerator at 20 ft. intervals.

Bending magnets and quadrupoles in the loops will be supported by simple metal stands which extend to the floor of the housing. Horizontal and vertical adjusting screws will be provided. Adjacent ends of neighboring magnets will be held by a single common support.

Alignment of the transport elements in the loops will be accomplished by precision surveying techniques. The centerlines of the various devices will be accurately referenced to targets (e.g., "tooling balls") mounted on their exterior surfaces. A large fraction of the surveying will be accomplished above ground and the alignment criteria will be translated to the transport elements by off-set techniques similar to those used in the alignment of the SLAC Beam Switchyard components.

4. Radiofrequency System

The radiofrequency system will consist of two conventional accelerator sectors capable of providing 150 MV per turn at a repetition rate of ~43.5 kHz. These extra sectors will be installed parallel to the present Sectors 21 and 22. For the accelerator proper, use will be made of spare disk-loaded waveguide and surplus Mark III sections from the Stanford High Energy Physics Laboratory. As discussed above, the new accelerator sections will be installed in the present housing, above the existing accelerator, high enough to clear all existing components (see Fig. 12). A total of 64 ten-foot sections mounted on 16 girders will be used.

The rf power will be supplied by 16 klystrons located in the klystron gallery. Each klystron will supply 220 kW of peak pulsed power to four sections on a girder. The klystron repetition rate will be ~43.5 kHz, i.e., one pulse every 23 μsec,

corresponding to the revolution frequency of the beam. As in the present accelerator, each pulse will be 2.5 μsec long giving a duty cycle of 10.9%. The average rf power per klystron will be ~24.2 kW. Each klystron will be powered by a modulator using a tetrode switch tube and a 1 μf, 45 kV storage capacitor. The waveguide feed system from the klystrons to the accelerator sections will be very similar to the existing rectangular waveguide system and will use the same vertical penetrations. The drive and phasing systems will conceptually resemble the existing systems but will have to accommodate the higher repetition rate and lower drive power. The entire radiofrequency system will require about 1 MW of additional electrical power.

5. Injector and Positron Source

The present SLAC injection system uses two electron guns, the first on axis, the second off axis; both are located upstream of the first accelerator section in Sector 1 and are operable interchangeably on a pulse-to-pulse basis. In the proposed layout for the recirculation system, the on-axis gun will be removed so that the beam can be reinserted directly into the accelerator. The off-axis gun will remain at its present location and operate as usual. For reliability purposes, the present on-axis gun might be remounted off-axis in the same area.

In addition to these modifications, a new off-axis injector will be installed in the first third of the accelerator, at about Sector 6. The beam from this injector will be used when a 17.5 GeV beam is desired on the first pass. On the second pass, 2.8 msec later, this beam will then receive the full acceleration of ~25 GeV for a total of 42.5 GeV. Simultaneously, a new beam will again emerge from the off-axis injector, thereby preserving the 360 pps repetition rate.

By reversing the magnetic field in all the recirculator magnets, it should also be possible to store and double-accelerate a positron beam. Since the present

maximum energy of positron beams (~ 14 GeV) is lower than the maximum recirculating energy, the maximum final positron energy will also be lower (~ 39 GeV). Furthermore, since the positrons are produced by means of a primary electron beam in Sector 11 and a 180° phase reversal beyond that point, it will not be possible to have positrons and electrons simultaneously in the accelerator and the maximum repetition rate will be 180 pps.

6. Vacuum System

The vacuum system envelope will follow the general outline of Fig. 7. The design of this system seems fairly straightforward except for one uncertain factor: the outgassing rate of the vacuum chamber due to synchrotron radiation. Indeed, the ~ 100 kW of power transferred to the beam by the radiofrequency system will reappear as synchrotron radiation in the loops.

The present design is expected to maintain an average pressure of 5×10^{-7} torr during storage time. The vacuum chamber will be made of aluminum in the curved sections and of stainless steel in the straight sections. The aluminum chamber will be extruded and have an elliptical cross section to conform to the A.G. magnet poles. Approximately 95 small ion pumps (~9 liters/sec) will be appropriately distributed along the recirculator so as to provide the required average pressure.

7. Electrical Utilities

The total additional power requirement for the recirculation system operating at 17.5 GeV is ~ 6.3 MW. The capacity of the main substation is more than adequate to supply this incremental load.

Taps will be provided at Sectors 3 and 5 to divert 12 kV power to 4 new substations located around the west-end loop. These substations will be of the outdoor type and will transform the power from 12 kV to 480 V. At the east end, power

will be taken from the beam switchyard substation and distributed to 4 outdoor-type substations located around the east-end loop. The 12 kV cables will be buried underground.

Power to the radiofrequency system (~1 MW) will be supplied from the 12 kV line at Sectors 21 and 22.

Power supplies for the magnets will be located in small above-ground shacks at each loop. Penetrations will carry dc power from the power supplies to the magnets located in the tunnel.

8. Cooling Water

Cooling water for components in the east-end loop will be supplied from the existing 1701 cooling tower (located near the beam switchyard). Water for components in the west-end loop will be supplied from cooling tower 1201 (located opposite Sector 9) which will be up-graded. The cooling of components in the two-mile accelerator housing in Sectors 21 and 22 will be handled by cooling tower 1202 (located opposite Sector 22).

9. Extraction, Inflection, Reinsertion, Long Spill, and Modified BSY Systems

The general principles of these systems have been illustrated in Fig. 7. For beam storage, once at the beginning of each 1/360th of a second, the 12-17.5 GeV beam must be extracted from the accelerator and inflected (by the Inflection system) into the east-end loop. At the end of this period, for energy doubling, it must be re-inserted into the injector end of the accelerator (by the Reinsertion system). For long-duty cycle operation, reinsertion is of course not needed but a "long-spill" magnet system will be installed close to the end of the accelerator. By building all these systems upstream of the existing BSY, the modifications in the BSY can be kept reasonably simple. Of course, a number of BSY magnets will have to be up-graded to accommodate the higher energies.

10. Shielding and Radiation

The shielding problems are concerned mainly with limiting the flux of neutrons and muons at the shield surface and at the project boundary. The shielding configuration (combined with operational interlocks and procedures) will limit the radiation at the project boundary to 5 mrem per year. An upper limit of 1.5 rem per year will be maintained for the radiation workers (this is 1/3 of the allowable level set by the AEC).

At the present time, it is planned to use about 15 ft. of earth shielding over the entire recirculation loop. Radiation measurements will then be made and any "hot spots" which are found will be remedied by realignment of the beam transport components, by changes in operating procedures, or by addition of localized shielding. The protection system must be designed with the capability of shutting off the beam within 1 to 2 pulse intervals (2.8 - 5.6 msec) in case the beam monitoring devices detect an out-of-tolerance radiation condition or in case the beam fails to complete its programmed recirculation schedule.

Calculations have been made for a 17.5 GeV, 10 mA, 100 kW beam. They indicate that the shielding and protection systems briefly described above should be able to maintain tolerable radiation levels for a continuous 1% beam loss (~1 kW) uniformly spread around the loop. Neutron dose should be extremely small while muon contribution should be entirely negligible. The calculations have also been extended to a 25 GeV, 10 mA, 150 kW beam. The average doses at this higher level will also be negligible. Additional localized shielding might be added if measurements detect any "hot spots."

11. Instrumentation and Control

Experience at SLAC with such systems as the injector, the positron source, sector control, etc., has shown that the best principle for good instrumentation

and control is to provide local controls for initial setup and troubleshooting but to centralize all the essential operational beam controls in the Main Control Center (MCC). In this manner, the local controls need not be manned on a full-time basis. The construction of the RLA will follow this general principle. There will be several subsystems to instrument:

a. The two new sectors with their 16 klystrons, modulators, drive and phasing systems in Sectors 21 and 22.

b. The two-mile long double-transport and beam guidance system.

c. The east and west-end loops with their magnets, power supplies, utilities, pumps, beam current and position monitors, personnel and machine protection systems, and radiation monitoring.

d. The loop inflection, reinsertion and long-spill systems and the modified BSY switching system.

Subsystems (a) and (b) will require controls very similar to existing accelerator instrumentation. The loops (subsystem (c)) may just have a few local instrumentation "alcoves." Subsystem (d) will be combined with present injector I/C and BSY I/C respectively.

The I/C system which will require the greatest ingenuity and innovation will be the beam guidance console display in MCC. This console display might be patterned after existing machine displays such as the lin Q, x, y, displays at SLAC or similar systems at other labs. The main difference between the new system and the existing one is that the beam will come around every 23 μsec and will have to "survive" 122 revolutions. Diagnostics will have to be devised to follow the beam around and to pinpoint not only at what point but also on what turn a particular beam parameter has been exceeded. Ovbiously, some sort of computer assistance will be required. Hopefully, the existing PDP-9 and SDS-925 computers will be adequate for this purpose.

IV. BEAM DYNAMICS

A. General Characteristics

The beam dynamics of the RLA generally resemble the dynamics of the Cornell Electron Synchrotron[4] with a few outstanding differences:

1. Since the energy and all the magnetic fields are held constant, the problem of moving the beam through the transition energy does not exist. The electron bunches will normally be located on the falling side of the rf wave.

2. Because the recirculator contains about 6000 meters of straight drift length with fairly closely spaced quadrupole lenses, it is possible to make adjustments in the betatron tune without affecting the bending system.

3. The reverse bends provide a continuous adjustment on the momentum compaction, $\alpha = \frac{\delta \ell}{\ell} \frac{E_0}{\epsilon}$. Here $\delta\ell/\ell$ is the fractional change in path length in the entire system due to the fractional change in energy ϵ/E_0; E_0 is the nominal energy of the stored beam. Normally α would be very small, i.e., $10^{-5} < \alpha < 2 \times 10^{-4}$. The low value for α is necessary to keep the short bunch length which must be preserved if the beam is to have a reasonable energy spectrum after the second acceleration pass.

4. The long drift length reduces the rf power required by reducing the relative time the beam spends in the bending magnetic field. Since the storage period is only 2.8 msec, the effect of the long path is to reduce the number of revolutions to the relatively small value of about 122.

B. Recirculating Lattice

1. Main Bends

The main bend lattice is expected to consist of alternating gradient cells. In order to reduce the driving of radial phase space blow-up by synchrotron quantum

fluctuations, it is desirable to reduce the rms value of the η-function. The η-function defines the off-momentum equilibrium orbit. This reduction is achieved by using magnets with high gradients. This yields a short betatron wavelength, resulting in short cells, each containing only two magnets.

Numerous alternative cells have been investigated by means of the TRANSPORT[5] and SYNCH[6] computer programs. The properties of a promising looking main bend lattice are summarized in Table III. Each cell contains two 3^{o} bending magnets: one focusing with index n=-900 and one defocusing with index n=+700. The mean field is 6.58 kG at 17.5 GeV. Figure 13 shows the function η, and the betatron functions β_x and β_y. The rather high gradient index of 900 has been shown by calculations to be within the practical upper limit imposed by magnet design at fields up to 9.4 kG. This is the highest equilibrium guide field proposed, corresponding to 25 GeV recirculation.

2. The η-Matching Sections

The matching of the η-function between the main bends and the adjacent straight sections is accomplished by a system consisting of a bending magnet which disperses the beam and a quadrupole which focuses the dispersed off-momentum rays.[7] With proper choice of spacing of the elements and quadrupole strength, the proper values of η and η' in the bending ring are matched to the condition $\eta = \eta' = 0$ in the straight sections. The overall transformation through the main bend is then achromatic, and $\overline{\eta^2}$ is minimized within the bending lattice. The proposed system as designed by use of TRANSPORT is shown in Fig. 14. Note that the main bend terminates in a full-length D-magnet (radially defocusing) at each end. The 1.5^{o} bending of each η-matching magnet then makes the total bend of the system an integral multiple of 6^{o}.

3. Reverse Bends

The reverse bends, in addition to their obvious function of bending the beam into and out of the main accelerator housing, serve the additional purpose of

providing a continuous adjustment of the momentum compaction. The reverse bend layout is shown in Fig. 15. The four 7.5^{o} bends each consist of three 2.5^{o} magnets. The system is symmetric about the central "symmetry" quadrupole. To understand the momentum compaction adjustment, refer to the dispersion ray diagram in Fig. 15. The off-momentum ray is focused by the doublet and passes through the central bend with negative dispersion — i.e., inside the mean ray. The symmetry quad symmetrizes the off-momentum ray, thus making the overall system achromatic. By varying the horizontal focal length of the doublet, the total path length difference given by

$$\delta\ell(\epsilon/E_0) = \int x(\epsilon/E_0)\,\frac{ds}{r}$$

may be varied over a finite range. Each of the main bends contributes about 1.1 m to this matrix element. Thus, for a design value of $\langle \delta\ell \,|\, \epsilon/E_0 \rangle \approx 0.7$ m for the entire recirculator, the matrix element for each reverse bend should be $\langle \delta\ell \,|\, \epsilon/E_0 \rangle \approx -0.75$ m. This corresponds to a momentum compaction of $\alpha = \langle \delta\ell \,|\, \epsilon/E_0 \rangle / L \approx 1 \times 10^{-4}$ (where $L \approx 6900$ m is the total path length). By using TRANSPORT, solutions have been found which are variable over a range of -0.75 ± 0.25 m, giving a net momentum compaction which may be varied within the range

$$3 \times 10^{-5} < \alpha < 17 \times 10^{-5}$$

The vertical focal strength of the doublets may be varied to keep the vertical transport properties of the system nearly constant.

Table III summarizes some of the transport properties of the entire recirculator. The numbers of betatron wavelengths are given in round numbers; in operation ν_x and ν_y will actually be set to avoid integer and half-integer resonances.

4. Damping Rates for Quantum-Fluctuations

The calculation of damping rates employs the damping factor D, defined by Sands[8] as

$$D = \frac{\oint \eta(s)\, G(s)\, [G(s)^2 + 2K_1(s)]\, ds}{\oint G(s)^2\, ds}$$

where the integrals are to be taken along the complete beam path. The function G(s) is

$$G(s) = 1/r(s) = \frac{ec}{E_0}\, B(s)$$

and the function $K_1(s)$ is the focusing term

$$K_1(s) = \frac{ec}{E_0} \left(\frac{dB(s)}{dx}\right)_0$$

evaluated on the design orbit, $x = 0$. The function $\eta(s)$ is the equilibrium orbit for an off-momentum particle:

$$x(s) = \eta(s)\, \epsilon/E_0$$

In terms of the gradient index n(s),

$$D = \frac{\oint \eta(s)\, G^3(s)\, [1 - 2n(s)]\, ds}{\oint G^2(s) ds}$$

The damping rates are given by $\alpha_i = J_i(fU/2E)$ where f is the circulating frequency and U is the energy lost per turn to synchrotron radiation. The coefficients J_i are the damping partition numbers given by $J_s = 2 + D$ for synchrotron phase oscillations and $J_x + J_y = 2 - D$ for the horizontal and vertical oscillations. As long as the J_i's are positive, the motion is damped. In the absence of x-y coupling, $J_y = 1$ and $J_x = 1 - D$. The recirculator will, however, have x-y coupling because of the tilted plane of the west loop. Thus, the damping partition number J_x will become less negative due to the x-y coupling. However, for the small values of

J_x that are anticipated, the antidamping rate is so slow as to be negligible during the 2.8 msec storage period for the energy range being considered. If the energy range of the RLA is increased in the future, it is possible to modify D by introducing special magnetic elements.

C. Rf System

1. Phase Stability

Phase stability in the RLA is achieved by placing the bunches of electrons on the falling side of the rf wave just as in a conventional synchrotron operating above the transition energy.

The farther the beam is phased off crest, the stronger the phase focusing becomes, but also the more peak rf voltage must be supplied. The synchrotron phase oscillations which result from quantum fluctuations in electron energy tend to be smaller in amplitude and more rapid as the bunches are phased farther off crest. However, the phase oscillations also depend on the momentum compaction parameter; the lower values of α result in smaller amplitude phase oscillations for the same energy excursion, but at a lower synchrotron oscillation frequency. These inter-relations are shown in Table IV[9] for the case of 17.5 GeV. Since the initial spread in phase and energy ($\epsilon_0/E_0 \approx 0.3\%$, $\delta\phi_0 \approx 4^o$) will likely be less than the damped values shown, and since the storage time is comparable to the synchrotron damping period, it is probable that the resultant phase and energy amplitudes will be less than those shown in Table IV.

2. Beam Loading

The steady-state beam loading voltage induced in a constant gradient accelerator section, with length ℓ, voltage attenuation parameter τ, shunt impedance per unit length r, and peak current i_p, is[10]

$$V_b = \frac{i_p r \ell}{2} \left[1 - \frac{2\tau e^{-2\tau}}{1 - e^{-2\tau}} \right]$$

For a SLAC section with $\tau = 0.57$, $\ell = 3.0$ m, r = 53 megohms/m, the beam loading voltage is calculated to be 0.037 MV/mA per section. For a conventional rf system using two sectors of SLAC structure (64 sections), the total beam loading voltage is 2.37 MV/mA. This steady-state value is attained after the 0.8 μsec transient, i.e., the structure filling time. It is possible to compensate for this transient by delaying the rf pulse of some of the klystrons during the filling time. This method is similar to the technique used regularly on the two-mile accelerator. If compensation for transient beam loading is done imperfectly, the bunch centroids will execute phase oscillations whose amplitudes must be added to the amplitudes of the phase oscillations within the bunches to determine the effective bunching of the stored beam.

The amount of current that can be recirculated is maximized if, after the transient effects have died out, all the klystrons are identically phased. From Fig. 16, the expression for the synchronous phase angle is

$$\tan \phi_s = \left[\frac{V_g^2 - (V_b + V_s)^2}{V_s^2} \right]^{1/2}$$

where V_g is the amplitude of the unloaded voltage produced by the klystrons, V_b is the amplitude of the beam induced voltage and V_s is the voltage required to replace synchrotron radiation losses. The effective rf voltage is the vector sum $\vec{V}_{rf} = \vec{V}_g + \vec{V}_b$ at a phase angle ϕ_s from the electron bunch so that $V_s = V_{rf} \cos \phi_s$. By solving for V_b yielding

$$V_b = \left[V_g^2 - V_s^2 \tan^2 \phi_s \right]^{1/2} - V_s$$

it is possible to calculate the maximum amount of beam loading for any phase angle. The last column in Table IV lists the peak recirculating current for the 17.5 GeV case assuming $V_g = 150$ MV. It shows that for a reasonable quantum lifetime of

~ 1 second, about 7 mA can be recirculated at $\alpha = 0.5 \times 10^{-4}$. At a lower recirculating energy, using the full 150 MV of rf voltage, it is possible to recirculate considerably more current up to the point where loading in the main accelerator becomes the limitation. Thus, for example, at 17.0 GeV, over 10 mA can be recirculated and at 15.0 GeV, over 30 mA can be recirculated. This latter value approaches preliminary estimates of the threshold of beam breakup in the recirculator.

D. Tolerances

1. Alignment Tolerances

Alignment tolerances have been calculated for the main bend loops with the assumption that the design consists of a 480° ring of A.G. magnets as described earlier. Since steering is neglected, this approach should be conservative. More detailed calculations of the actual configuration are in progress.

The most sensitive tolerances are for beam position due to transverse errors in the magnet position (Δx and Δy) and for rotation of the magnet about the beam axis ($\Delta\phi_z$). As compared to the tolerances calculated for the lower gradient structure built at Cornell,[4] the tolerances for Δx and $\Delta\phi_z$ are tighter by a factor of less than 2, i.e., more than half the allowable error. The tightest tolerance is the vertical displacement Δy, which is almost three times tighter than the Cornell tolerance for the circular model. Special care in mounting adjacent magnets to a common stand is expected to satisfy this tolerance requirement which is approximately 0.1 mm; the actual numbers remain to be determined. Vertical steering, which can be provided in the main bend loops, will substantially relax the vertical alignment tolerance.

2. Magnet Tolerances

Magnet tolerances, including field and gradient tolerances, have been calculated using the same model ring. The tolerance on gradient errors needs to be determined on the basis of the second order isochronous (sextupole) correction to the pole face of the gradient magnets. The tolerance on $\oint$Bdl can be met by grouping magnets of similar $\oint$Bdl on the same power supply. Each power supply is expected to power about twelve to fourteen 3^{o} gradient magnets. The regulation required of the power supplies is 0.1%, which is substantially less than the expected momentum spread of $\approx$0.3%.

E. Instabilities

The following instabilities and special beam problems have been studied:

1. X-Y Coupling

An analysis has been made to study the effects of x-y coupling upon the damping rates of the x-y oscillations. The results show that as the coupling increases, the larger of the two damping rates decreases and the smaller of the two damping rates increases. In the limit of very large coupling, the two damping rates become equal and are given by the average value of the damping rates for the noncoupled case. For the case of small coupling, the change in the damping rate is proportional to the square of the coupling.

2. Tune-Shift Due to Energy Spread

The betatron oscillation tune shifts $\Delta\nu_x$ and $\Delta\nu_y$ for the off-momentum particles have been calculated for the proposed magnet lattice. The calculations confirm that it is important to include a sextupole correction in the alternating gradient magnets. The effect is to make the betatron tune in the main bends independent of energy. Similar corrections in the reverse bends, where zero gradient magnets are planned, can be provided by small individual sextupole magnets.

3. Head-Tail Effect

The growth rates for the head-tail instability have been calculated. In this calculation the value of the coupling impedance and the chromaticity are assumed to be comparable to those of Adone. The threshold for this instability depends on the tune shift due to energy spread. Even without the sextupole correction described above, the threshold appears well above the design current for the RLA.

4. Betatron Frequency Shift Due to Ion Neutralization

The betatron oscillation frequency can be shifted by the neutralization of the electric space charge forces by residual ions. Calculations assuming complete neutralization, leaving the self-magnetic field of the beam uncancelled, show a negligible shift in betatron tune. Thus for currents in the range proposed, i.e., 10-30 mA, the vacuum requirements for the RLA are based on scattering of the beam and are not made more stringent because of residual ions.

5. Synchrotron Frequency Shift Due to Space Charge

The synchrotron frequency shift from space charge has been estimated assuming that the beam current density decreases quadratically with distance from the center of the bunch. Under typical operating conditions of current, accelerator gradient and phase angle, this effect was found to be negligible.

6. Effect of RF Amplitude and Phase Jitter

Pulse-to-pulse jitter in the amplitude and phase of the RLA klystrons will produce coherent stochastic growth of synchrotron oscillations, resulting in uncertainty as to the final phase angle of the bunch. Linearized synchrotron dynamics have been used to estimate this effect. On the assumption that the uncertainty in final phase should be less than 5^{o}, the tolerances turn out to be about 1.1^{o} in phase and 1.1% in amplitude for jitter which is coherent in all 16 klystrons; or about 4.5^{o} in phase and 4.5% in amplitude for jitter which is uncorrelated between klystrons.

7. Beam Breakup Due to Transverse RF Mode Excitation

Beam breakup can occur in the RLA because of transverse interaction of the beam with the HEM_{11} mode in the accelerating structures. The transverse interaction with the recirculator linac is cumulative during the storage period. However, the recirculation time (23 μsec) is long compared to both the decay time of the rf fields (1 μsec) and the beam pulse length (1.6 μsec). Consequently, the structure has no "memory" from one beam passage to the next; information is carried only by the beam.

An approximate analysis of this effect has been made. A preliminary calculation indicates that the breakup threshold is on the order of 30 mA. In practice, this threshold may be raised by selective detuning of the RLA accelerator structures and by the phenomenon of Landau damping. Furthermore, since the total storage time is comparatively long, it would be possible to use feedback to control the effect.

V. SCHEDULE

The following Table displays the design, construction, installation and testing schedule for the Recirculating Linear Accelerator. Note that the total schedule extends over a period of three fiscal years from time of authorization to operation.

TIME SCHEDULE

RECIRCULATING ACCELERATOR

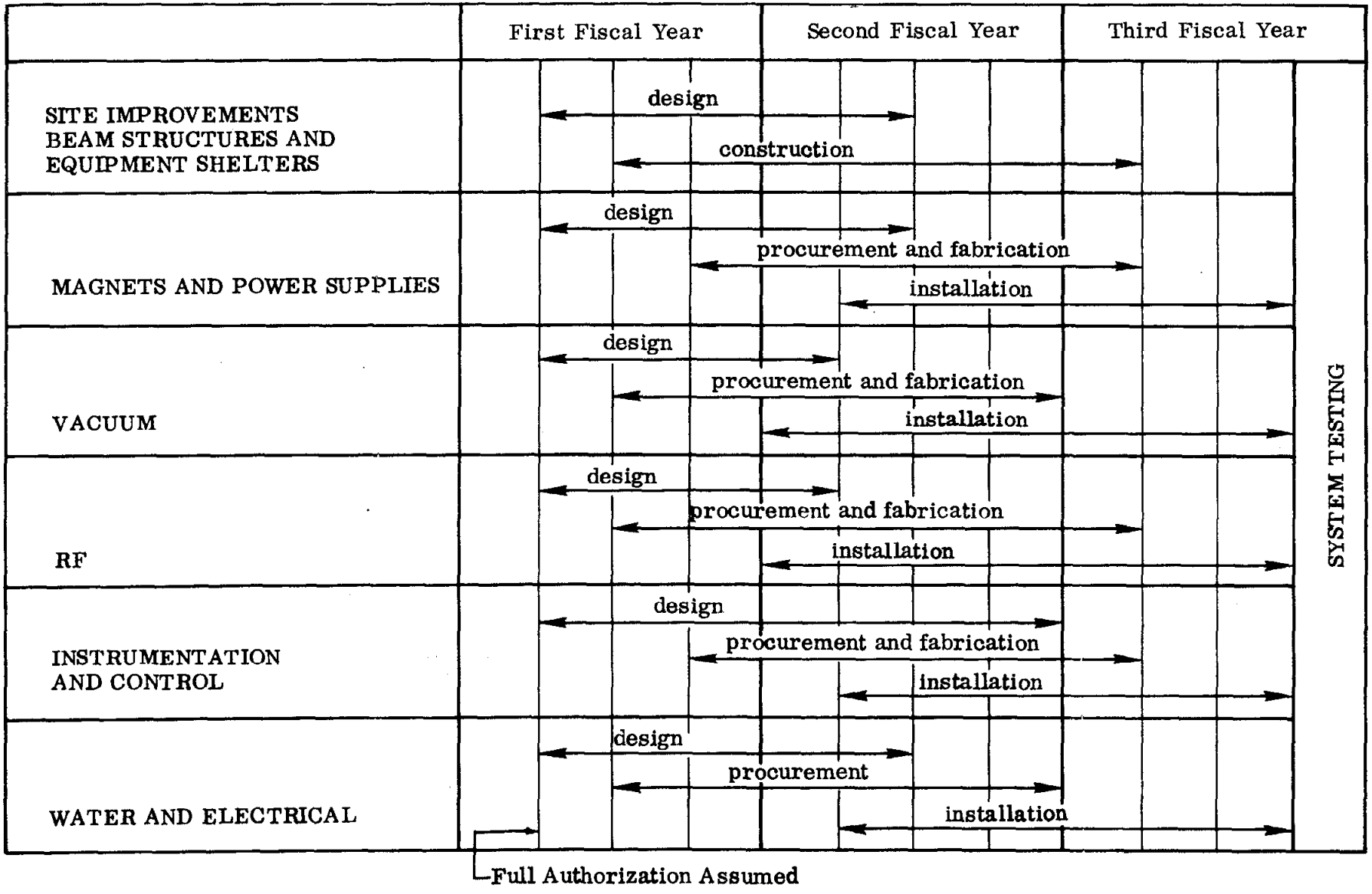

REFERENCES

1. P. B. Wilson, R. B. Neal, G. A. Loew, H. A. Hogg, W. B. Herrmannsfeldt, R. H. Helm and M. A. Allen, "Superconducting accelerator research and development at SLAC," Particle Accelerators 1, 223 (1970).
2. W. B. Herrmannsfeldt, "Recirculating SLAC with a superconducting section," Report No. SLAC-TN-70-27, Stanford Linear Accelerator Center, Stanford, California (1970).
3. W. B. Herrmannsfeldt, "Recirculating SLAC with a superconducting section, Part II," Report No. SLAC-TN-71-4, Stanford Linear Accelerator Center, Stanford, California (1971).
4. R. R. Wilson, "Cornell electron synchrotron," CS-33, Laboratory of Nuclear Studies, Cornell University, Ithaca, New York (1967).
5. K. L. Brown and S. K. Howry, "Transport/360," Report No. SLAC-91, Stanford Linear Accelerator Center, Stanford, California (1970).
6. A. A. Garren and A. S. Kenny, SYNCH, Internal Document, Lawrence Radiation Laboratory, Berkeley, California (1968).
7. P. L. Morton and J. R. Rees, "The design of the low-beta insertions for storage rings, IEEE Transactions In Nuclear Science (June 1967).
8. M. Sands, "The physics of electron storage rings, an introduction," Report No. SLAC-121, Stanford Linear Accelerator Center, Stanford, California (1970); p. 100.
9. J. R. Rees, "Radiation effects in a multi-GeV electron recirculator," Report No. SLAC-TN-70-20, (also an unpublished on-line computer program which was used for Table IV), Stanford Linear Accelerator Center, Stanford, California (1970).
10. R. B. Neal, editor, The Stanford Two-Mile Accelerator (W. A. Benjamin, Inc. New York, 1968); p. 118.

MAXIMUM VALUES OF VARIOUS PARAMETERS FOR THREE OPERATING MODES

	High Energy Mode[1]			High Duty Cycle Mode		A
Output Beam Energy (GeV)	42.5	46	60	17.5	25	
Recirculating Beam Energy (GeV)	17.5	21	25	17.5	25	
Beam Pulse Repetition Rate (pps)	360	360	180	4×10^4	4×10^4	:
Beam Pulse Length (μsec)	1.6	1.6	1.6	1.6	1.6	
No. of Electrons per Pulse ($\times 10^{10}$)	10	10	10	0.10	0.10	
Duty Cycle (%)	0.06	0.06	0.03	7	7	
Average Beam Current (μA)	6	6	3	6	6	
Average Beam Power (kW)	244	276	180	105	150	1(
Peak Output Beam Current (mA)	10	10	10	0.10	0.10	
Recirculating Beam Current (mA)	0.7	0.7	0.7	0.7	0.7	
Output rf Peak Power per Klystron (MW)	21	30	60	21	30	
RF Pulse Repetition Rate (pps)	360	360	180	360	360	:

(1) Parameters are given for final energies of 42.5, 46 and 60 GeV.

(2) Parameters are given for 30 MW and 60 MW output peak power per station.

TABLE II

SECONDARY PARTICLE YIELDS

Particle	Particles/sec
$\pi^{\pm}$	$\sim 10^6$
K^+	few $\times 10^4$
K^-	$\sim 10^4$
$\bar{p}$	few $\times 10^3$
p(n)	$\sim 10^4$
K^o_L	few $\times 10^4$

TABLE III

MAGNET LATTICE PARAMETERS

Number of Betatron Wavelengths (rounded to nearest integer):

	Main Bends	Straight Sections	Total (including misc.)
Horizontal	11 each	6 total	31
Vertical	5 each	6 total	19

Beam Path Lengths (6900 m total including miscellaneous):

Main Bends	Reverse Bends	Main Tunnel
2×375 m	2×154 m	3090 m east 2230 m west

Recirculator Period	Recirculator Frequency	Harmonic Number
23 μsec	43.5 kHz	6.6×10^4

Estimated beam size: ± 0.7 cm maximum radial and vertical.

Path length dispersion per 210^{o} bend: $\langle \delta \ell | \epsilon / E_0 \rangle = 1.125$ m.

Damping factor: $D = 1.56$

TABLE IV

SYNCHROTRON OSCILLATION PARAMETERS FOR 17.5 GeV

$U = 125$ MeV/turn $\qquad \mu_c = 134$ keV

$\alpha_0 = 157\ \text{sec}^{-1}$ $\qquad \alpha_s = 550\ \text{sec}^{-1}$

Synchrotron damping period = 1.8 msec

Momentum spread (at damped equilibrium) = 0.12%

V_{RF} (MV)	ϕ_s (degrees)	T_s (turns)	ϵ_m/E_0 (%)	σ_ϕ (degrees)	$T_{quantum}$ (msec)	i_p (mA)
		Momentum Compaction $\alpha = 0.5 \times 10^{-4}$				
130	16	30	.33	6.8	1.1×10^1	8.8
135	22	26	.54	5.7	3.0×10^3	6.9
140	27	23	.73	5.1	6.6×10^6	4.7
		Momentum Compaction $\alpha = 1 \times 10^{-4}$				
135	22	18	.39	8.0	3.1×10^1	6.9
140	27	16	.52	7.2	1.1×10^3	4.7
145	31	15	.63	6.7	8.7×10^4	2.1
		Momentum Compaction $\alpha = 1.5 \times 10^{-4}$				
140	27	13	.42	8.9	7.4×10^1	4.7
145	31	12	.52	8.2	1.2×10^3	2.1
150	34	11.5	.61	7.7	2.9×10^7	0.0

In this table, U is the energy lost per turn by synchrotron radiation and μ_c is the critical energy of the synchrotron radiation. The damping rates are given by $\alpha_0 = fU/2E_0$, where f is the recirculator frequency, and $\alpha_s = (2 + D)\alpha_0$. V_{RF} is the peak value of the RF voltage, ϕ_s is the synchronous phase angle and σ_ϕ is the standard deviation of phase angle. T_s is the synchrotron oscillation period and ϵ_m/E_0 is the momentum acceptance of the system. The quantum lifetime $T_{quantum}$ is the expected lifetime of an electron due to the possibility that a quantum fluctuation will excite phase (energy) oscillations out of the RF bucket. For negligible losses during the storage period, the quantum lifetime should be $T_{quantum} \gg 100\ T_s$, i.e., several hundred milliseconds. It can be seen that this condition is amply fulfilled for the higher peak voltages. The last column shows the peak pulsed current that can be recirculated assuming that the maximum unloaded RF voltage is 150 MV.

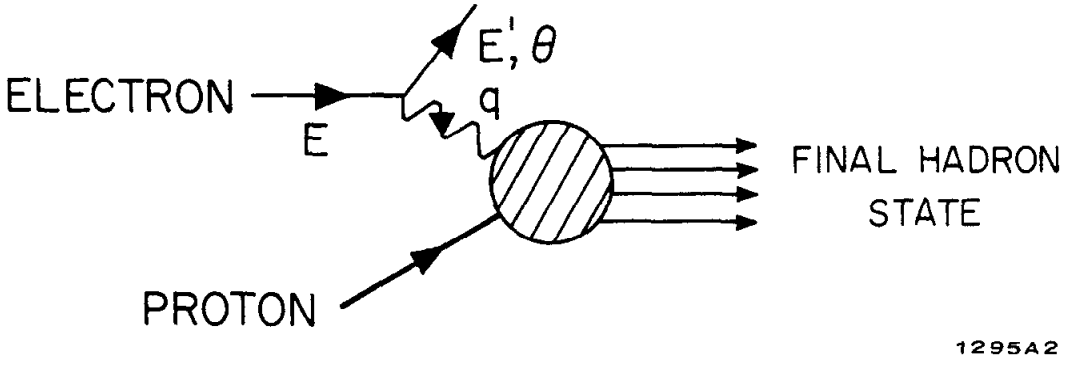

FIG. 1--Feynman diagram for inelastic electron scattering on protons. The laboratory energy of the virtual photon is $\nu = E - E'$, and $q^2 = 4EE' \sin^2 \theta/2$ is the square of the virtual-photon four momentum.

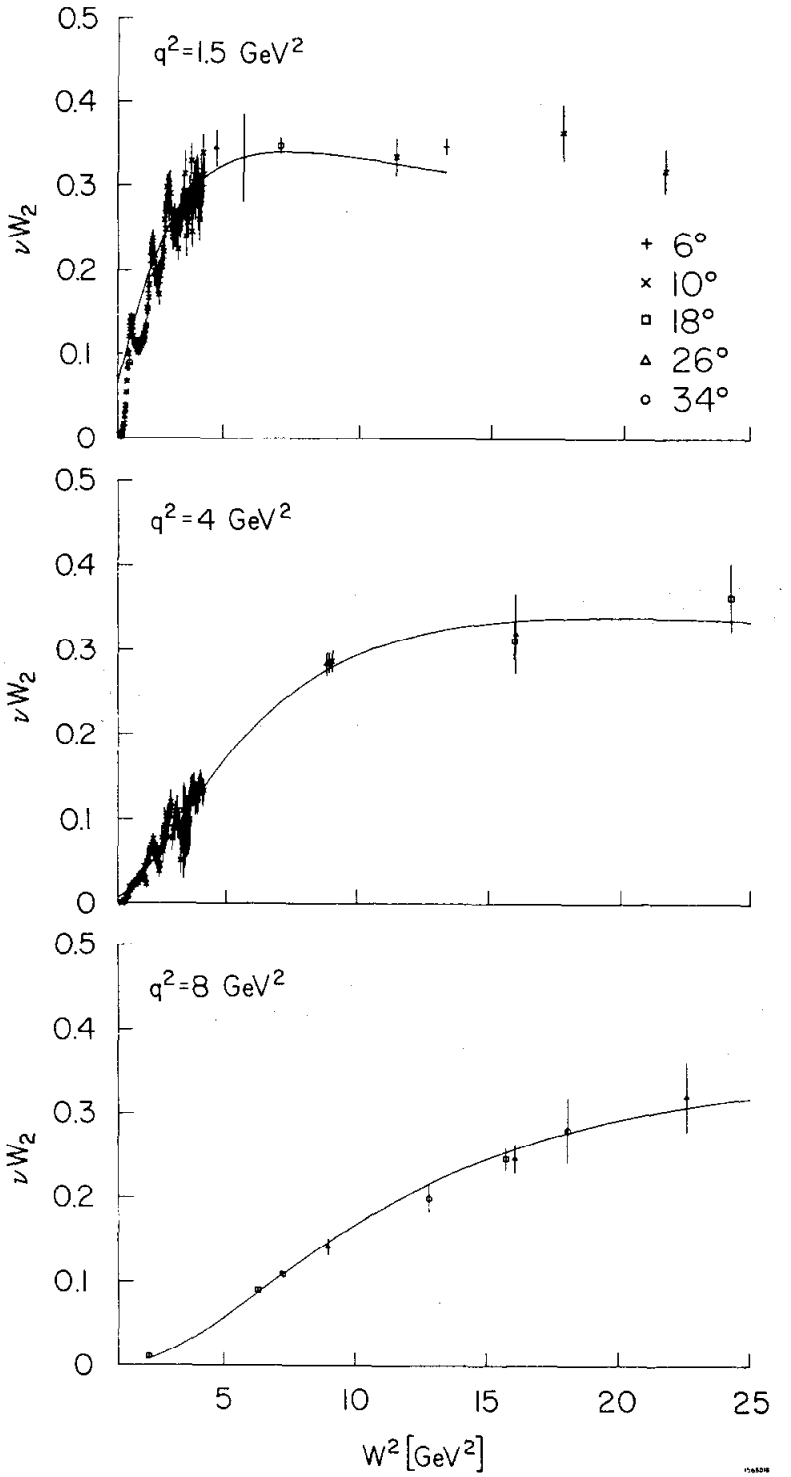

FIG. 2--Structure function of the proton from SLAC inelastic electron-proton scattering data. The horizontal scale is the square of the mass of the final hadron state $W^2 = M_p^2 + 2M_p\nu - q^2$. The laboratory cross section, in terms of the structure functions $W_1(\nu, q^2)$ and $W_2(\nu, q^2)$ and the electron scattering angle θ, is

$$\frac{d\sigma}{d\Omega dE'} = \frac{\alpha^2}{4E^2} \frac{\cos^2 \theta/2}{\cos^4 \theta/2} \left(W_2 + 2 \tan^2 \theta/2 \, W_1 \right).$$

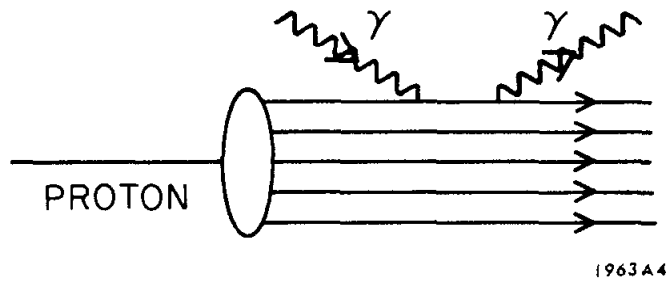

FIG. 3--Inelastic Compton effect from the proton with transfer of a large transverse momentum to the outgoing photon. The Compton scattering is from a "parton" constituent of the proton.

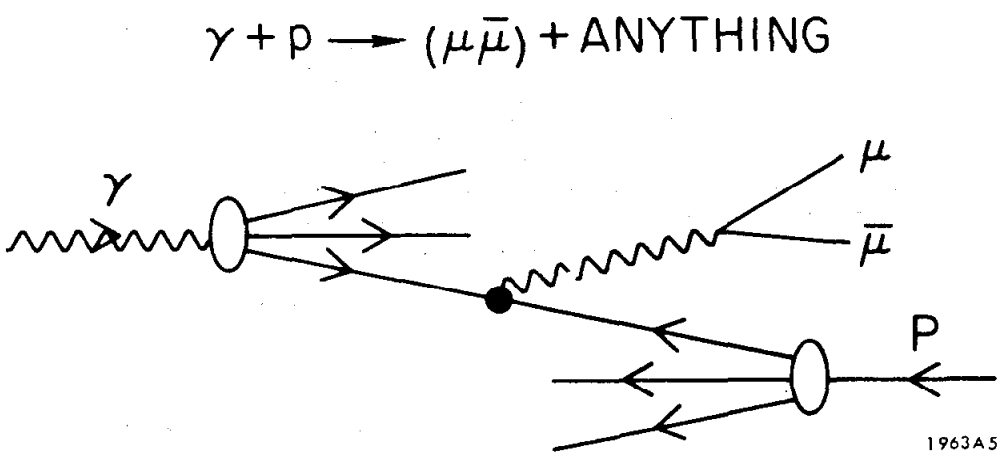

FIG. 4--Massive μ-pair production in a photon-proton collision. The mechanism is by annihilation of a parton-antiparton pair to form a massive virtual photon.

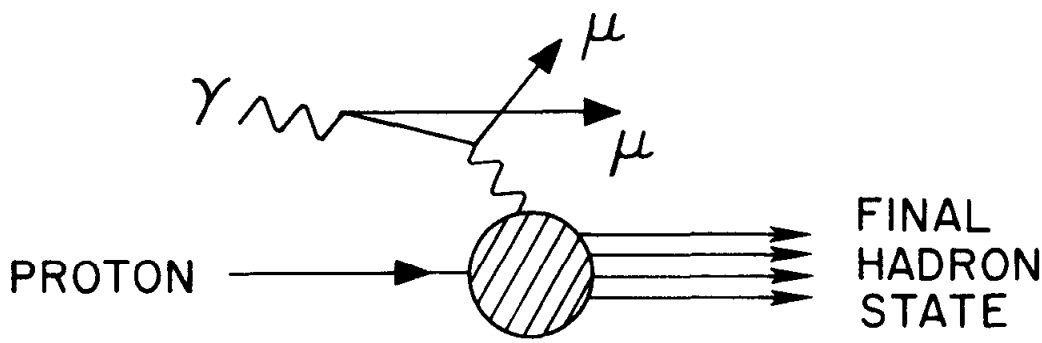

1295A1

FIG. 5--"Virtual" muon beam for inelastic scattering. Events are triggered on the unscattered (spectator) muons.

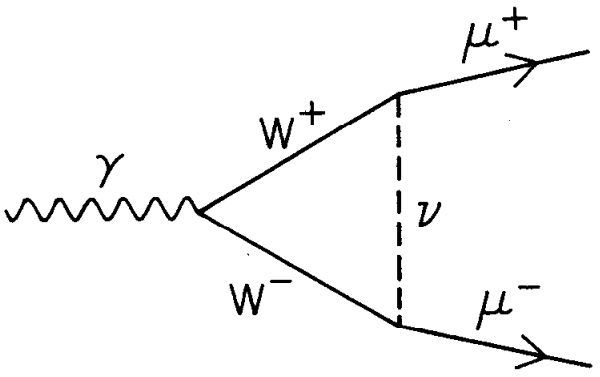

(a) OBSERVATION OF W PAIR PRODUCTION BY STUDYING μ PAIRS

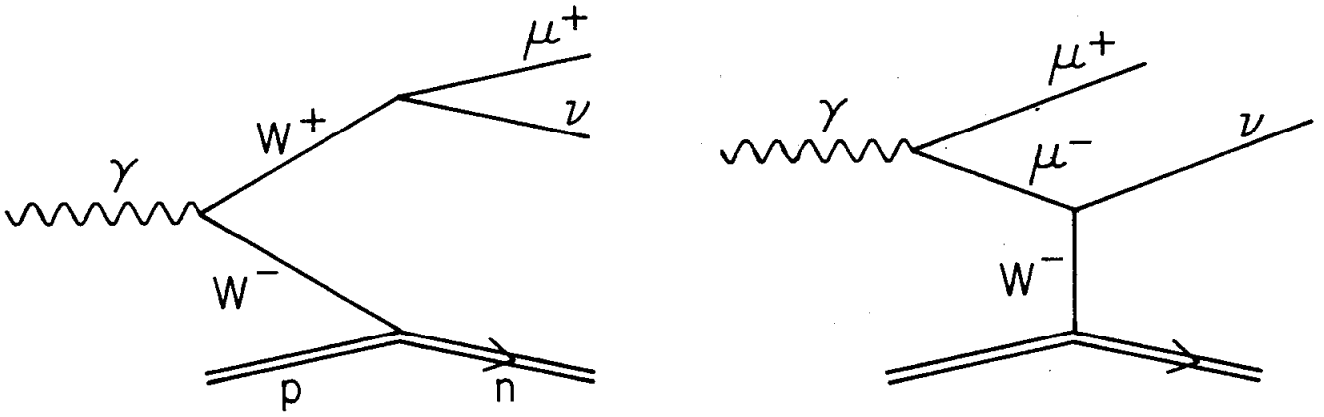

(b) OBSERVATION OF W PRODUCTION BY STUDYING SINGLE μ PRODUCTIONS

1963A6

FIG. 6

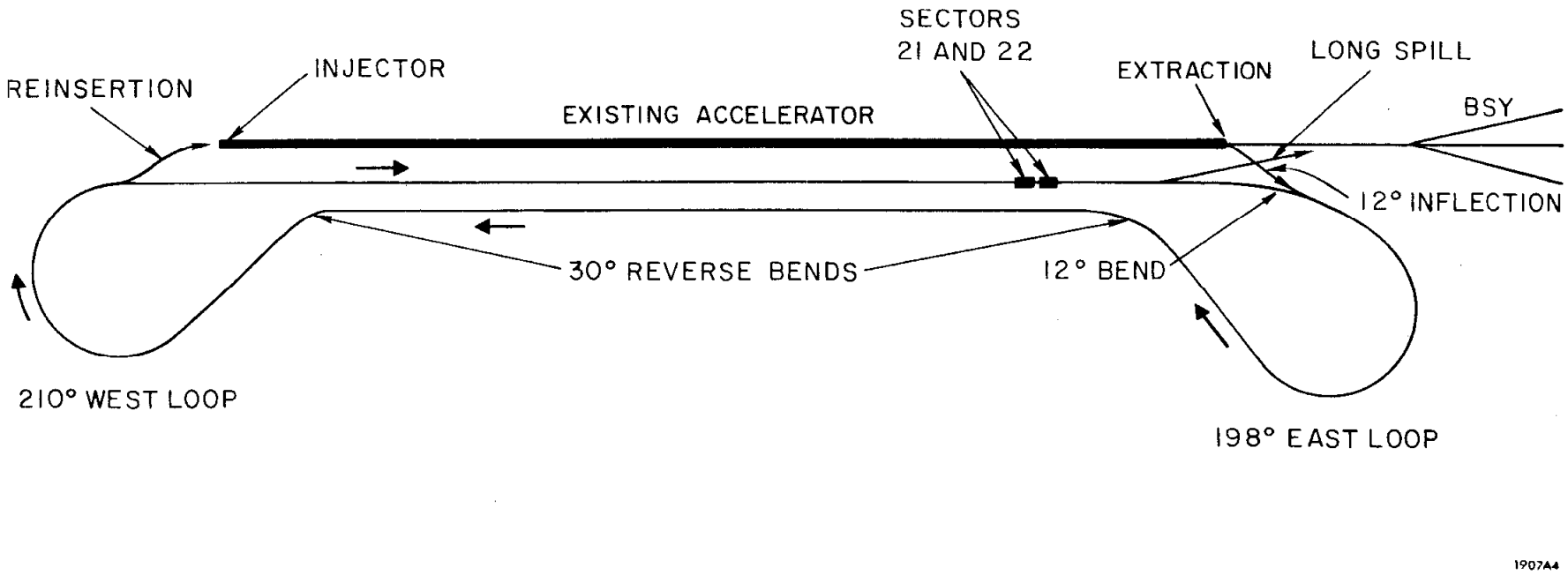

FIG. 7--Schematic layout of recirculation system.

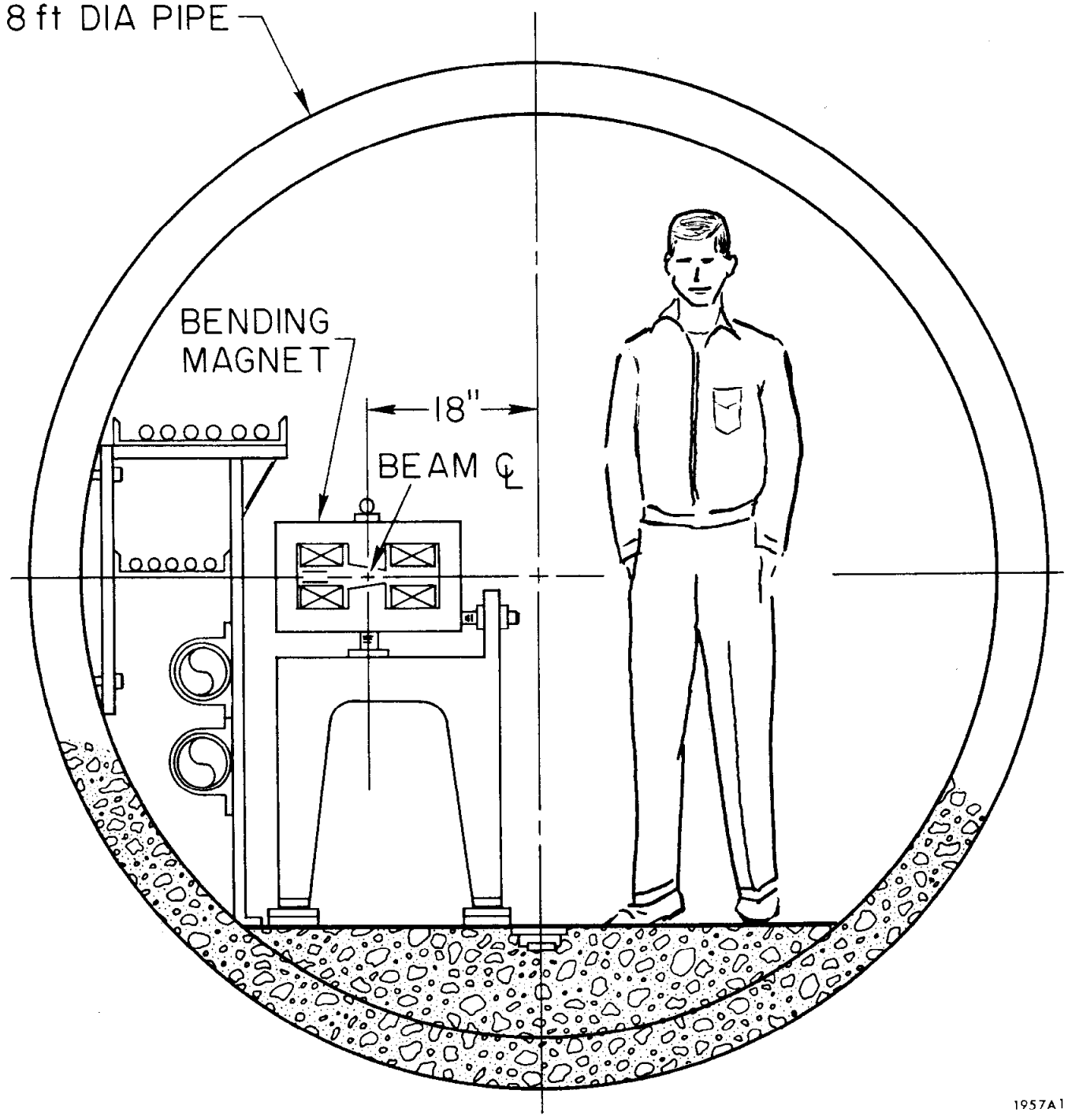

FIG. 8--Typical cross section of tunnel in the loops.

1748A4

FIG. 9--Aerial view of SLAC showing RLA layout.

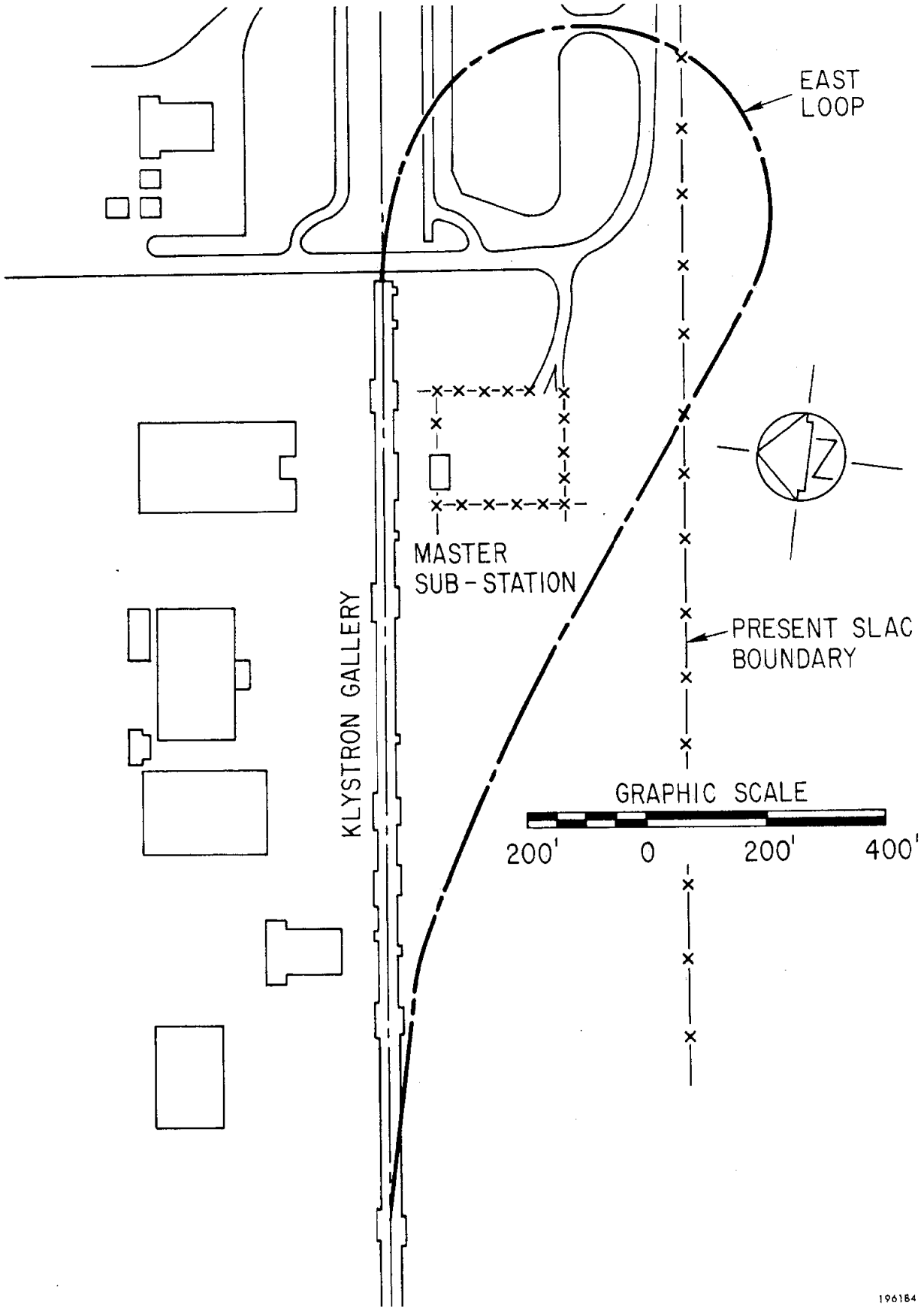

FIG. 10--Layout of East loop.

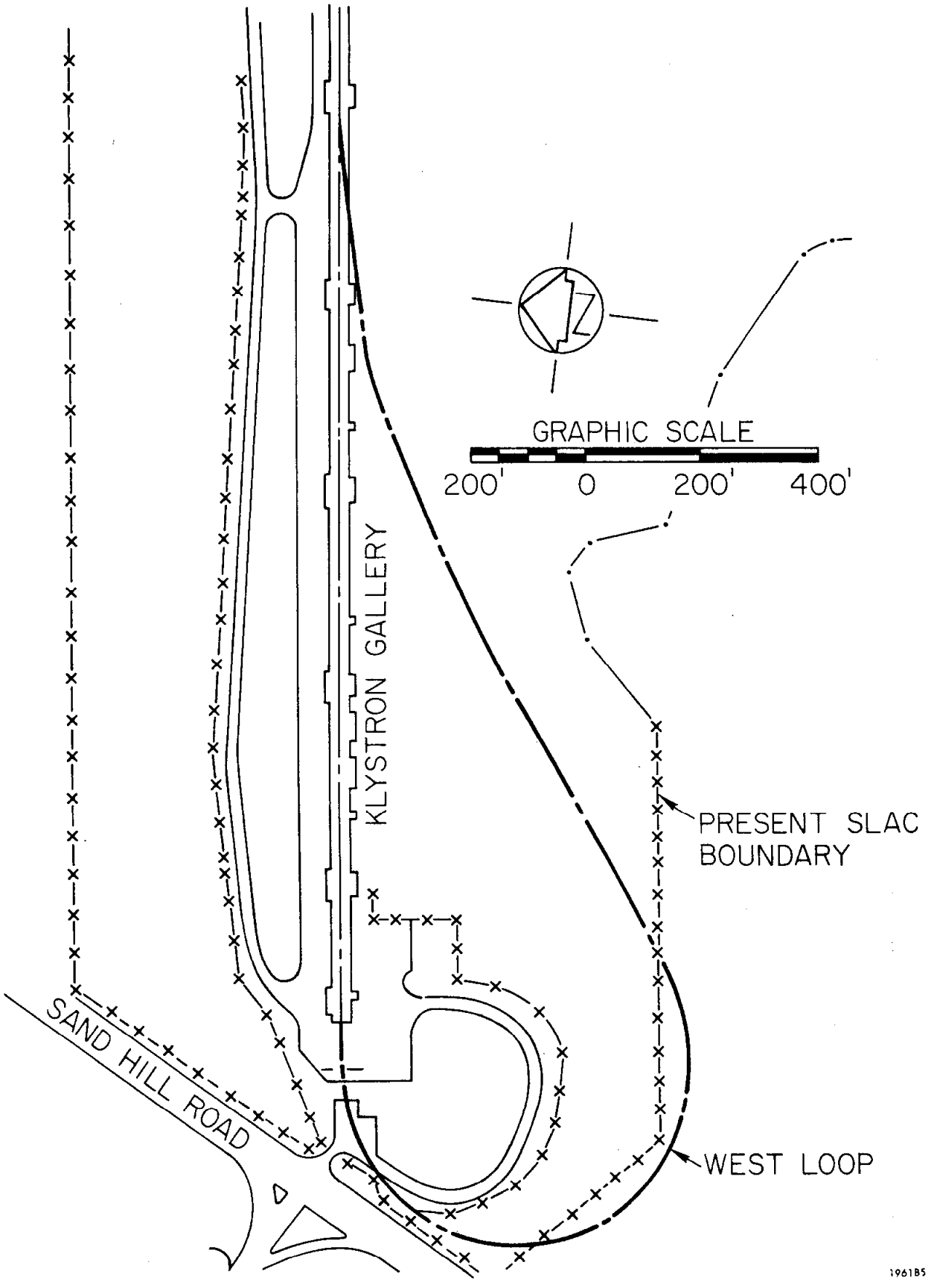

FIG. 11--Layout of West loop.

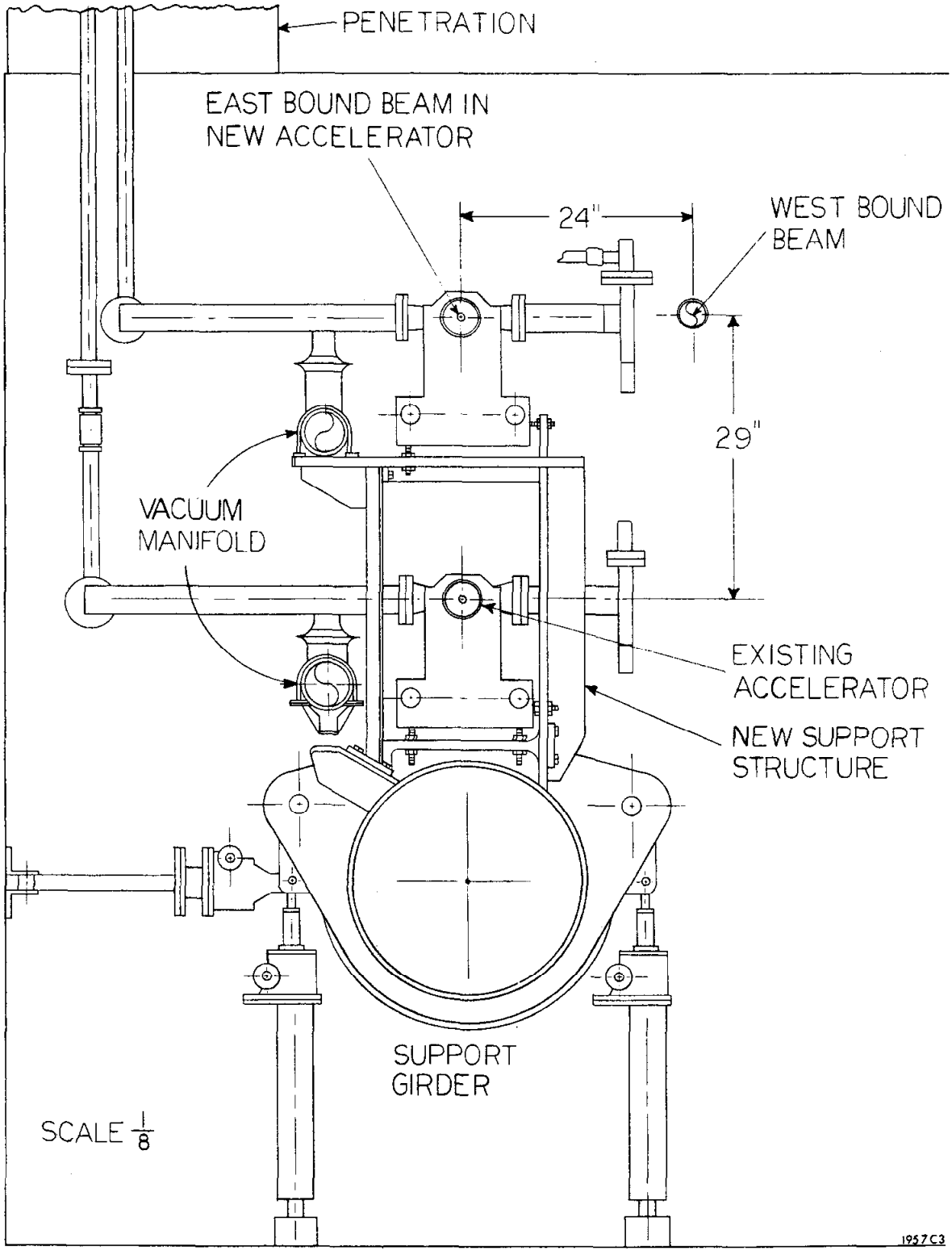

FIG. 12--Schematic of Accelerator Housing showing cross sections of present accelerator, 666 ft new accelerator (east-bound beam) and return loop (west-bound beam).

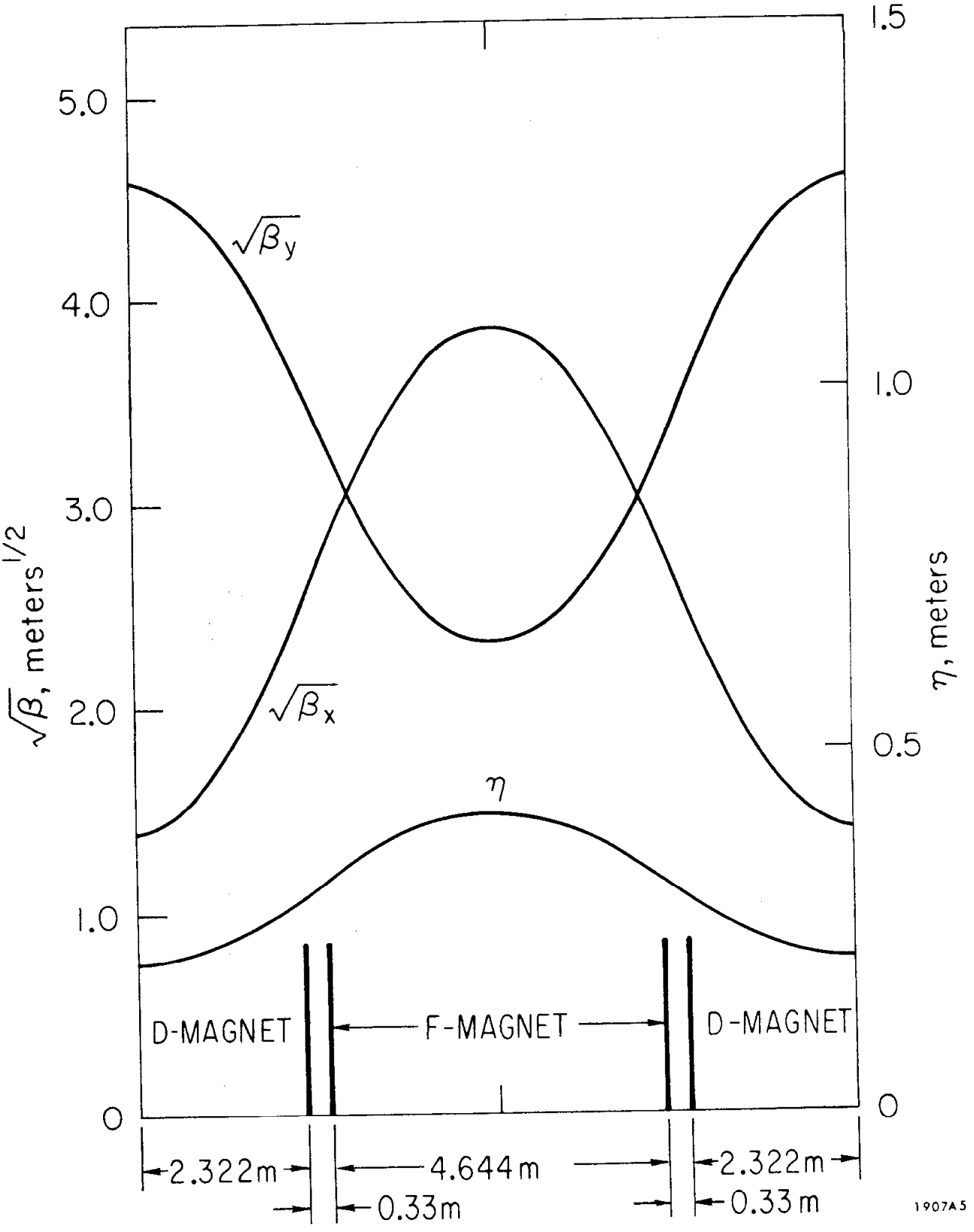

FIG. 13--η, β_x and β_y functions.

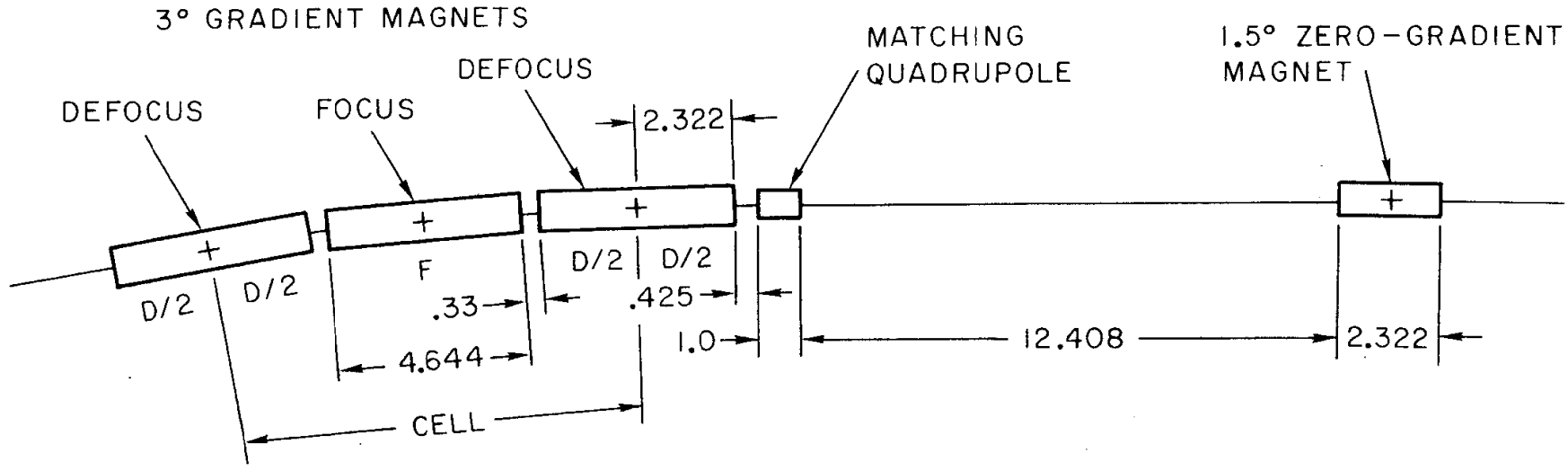

FIG. 14--Section of main ring showing η-matching section and one complete cell.

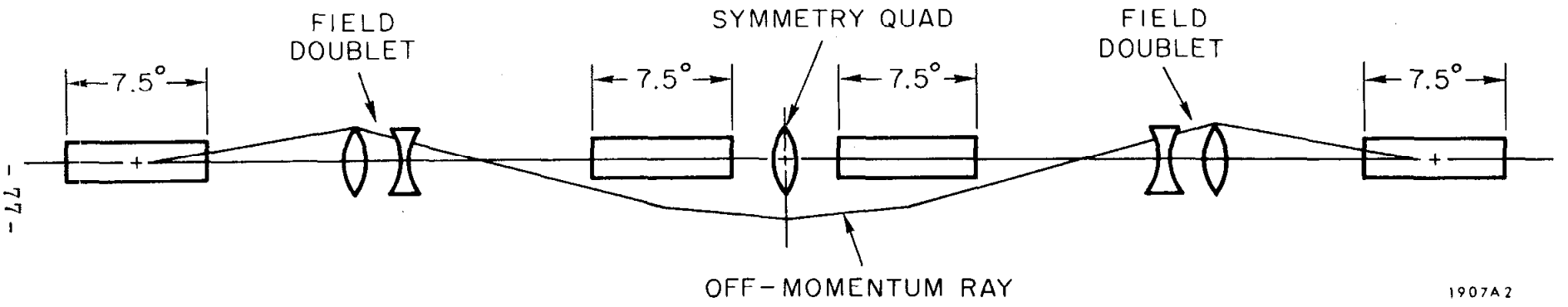

FIG. 15--Dispersion-ray diagram for reverse-bend system. Each 7.5° bend consists of three 2.5° magnets.

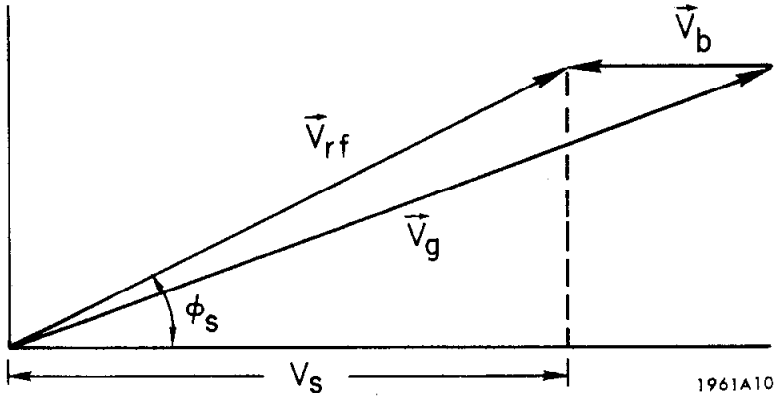

FIG. 16--Vector diagram showing the addition of the generator voltage V_g and the beam induced voltage V_b to result in the final rf voltage V_{rf} where ϕ_s is measured from the wave crest.